



OKLAHOMA TRANSPORTATION CENTER

ECONOMIC ENHANCEMENT THROUGH INFRASTRUCTURE STEWARDSHIP

ACCURATE VEHICLE CLASSIFICATION INCLUDING MOTORCYCLES USING PIEZOELECTRIC SENSORS

HAZEM REFAI, PH.D.

OTCREOS9.1-42-F

Oklahoma Transportation Center
2601 Liberty Parkway, Suite 110
Midwest City, Oklahoma 73110

Phone: 405.732.6580
Fax: 405.732.6586
www.oktc.org

DISCLAIMER

The contents of this report reflect the views of the authors, who are responsible for the facts and accuracy of the information presented herein. This document is disseminated under the sponsorship of the Department of Transportation University Transportation Centers Program, in the interest of information exchange. The U.S. Government assumes no liability for the contents or use thereof.

TECHNICAL REPORT DOCUMENTATION PAGE

1. REPORT NO. OTCREOS9.1-42-F	2. GOVERNMENT ACCESSION NO.	3. RECIPIENTS CATALOG NO.	
4. TITLE AND SUBTITLE Accurate Vehicle Classification Including Motorcycles using Piezoelectric Sensors.	5. REPORT DATE March 30, 2013		
	6. PERFORMING ORGANIZATION CODE		
7. AUTHOR(S) Hazem Refai, Ph.D.	8. PERFORMING ORGANIZATION REPORT		
9. PERFORMING ORGANIZATION NAME AND ADDRESS School of electrical and computer engineering University of Oklahoma-Tulsa 4502 E 41st St. Rm 4W139 Tulsa, OK, 74135	10. WORK UNIT NO.		
	11. CONTRACT OR GRANT NO. DTRT06-G-0016		
12. SPONSORING AGENCY NAME AND ADDRESS Oklahoma Transportation Center (Fiscal) 201 ATRC Stillwater, OK 74078 (Technical) 2601 Liberty Parkway, Suite 110 Midwest City, OK 73110	13. TYPE OF REPORT AND PERIOD COVERED Final July 2009 – March 2013		
	14. SPONSORING AGENCY CODE		
15. SUPPLEMENTARY NOTES University Transportation Center			
16. ABSTRACT <p>State and federal departments of transportation are charged with classifying vehicles and monitoring mileage traveled. Accurate data reporting enables suitable roadway design for safety and capacity. Vehicle classifiers currently employ inductive loops, piezoelectric sensors, or some combination of both, to aid in the identification of the 13 Federal Highway Administration (FHWA) classifications. However, systems using inductive loops have proven unable to accurately classify motorcycles and record pertinent data. Previous investigations undertaken to overcome this problem have focused on classification techniques utilizing inductive loops signal output, magnetic sensor output with neural networks, or the fusion of several sensor outputs. Most were off-line classification studies with results not directly intended for product development. Vision, infrared, and acoustic classification systems among others have also been explored as possible solutions.</p> <p>This project presents a novel vehicle classification setup that examines two approaches of using single- and multi-element piezoelectric sensors placed diagonally on the roadway to accurately identify motorcycles from among other vehicles, as well as identify vehicles in the remaining 12 FHWA classifications. An algorithm was formulated and deployed in an embedded system for field testing. Both single- and multi-element piezoelectric sensors were investigated for use as part of the vehicle classification system. The piezoelectric sensors and vehicle classification system reported in this project were tested at the University of Oklahoma-Tulsa campus and on Oklahoma state highways. Various vehicle types traveling at a variety of vehicle speeds were investigated. The newly developed vehicle classification system demonstrated results that met expectations for accurately identifying motorcycles, among other FHWA classes.</p>			
17. KEY WORDS Vehicle classification, motorcycle classification, piezoelectric sensor,	18. DISTRIBUTION STATEMENT No restrictions. This publication is available at www.oktc.org and from the NTIS.		
19. SECURITY CLASSIF. (OF THIS REPORT) Unclassified	20. SECURITY CLASSIF. (OF THIS PAGE) Unclassified	21. NO. OF PAGES 81 + covers	22. PRICE

SI (METRIC) CONVERSION FACTORS

Approximate Conversions to SI Units				
Symbol	When you know	Multiply by	To Find	Symbol
LENGTH				
in	inches	25.40	millimeters	mm
ft	feet	0.3048	meters	m
yd	yards	0.9144	meters	m
mi	miles	1.609	kilometers	km
AREA				
in ²	square inches	645.2	square millimeters	mm ²
ft ²	square feet	0.0929	square meters	m ²
yd ²	square yards	0.8361	square meters	m ²
ac	acres	0.4047	hectares	ha
mi ²	square miles	2.590	square kilometers	km ²
VOLUME				
fl oz	fluid ounces	29.57	milliliters	mL
gal	gallons	3.785	liters	L
ft ³	cubic feet	0.0283	cubic meters	m ³
yd ³	cubic yards	0.7645	cubic meters	m ³
MASS				
oz	ounces	28.35	grams	g
lb	pounds	0.4536	kilograms	kg
T	short tons (2000 lb)	0.907	megagrams	Mg
TEMPERATURE (exact)				
°F	degrees Fahrenheit	(°F-32)/1.8	degrees Celsius	°C
FORCE and PRESSURE or STRESS				
lbf	poundforce	4.448	Newtons	N
lbf/in ²	poundforce per square inch	6.895	kilopascals	kPa

Approximate Conversions from SI Units				
Symbol	When you know	Multiply by	To Find	Symbol
LENGTH				
mm	millimeters	0.0394	inches	in
m	meters	3.281	feet	ft
m	meters	1.094	yards	yd
km	kilometers	0.6214	miles	mi
AREA				
mm ²	square millimeters	0.00155	square inches	in ²
m ²	square meters	10.764	square feet	ft ²
m ²	square meters	1.196	square yards	yd ²
ha	hectares	2.471	acres	ac
km ²	square kilometers	0.3861	square miles	mi ²
VOLUME				
mL	milliliters	0.0338	fluid ounces	fl oz
L	liters	0.2642	gallons	gal
m ³	cubic meters	35.315	cubic feet	ft ³
m ³	cubic meters	1.308	cubic yards	yd ³
MASS				
g	grams	0.0353	ounces	oz
kg	kilograms	2.205	pounds	lb
Mg	megagrams	1.1023	short tons (2000 lb)	T
TEMPERATURE (exact)				
°C	degrees Celsius	9/5+32	degrees Fahrenheit	°F
FORCE and PRESSURE or STRESS				
N	Newtons	0.2248	poundforce	lbf
kPa	kilopascals	0.1450	poundforce per square inch	lbf/in ²

ACKNOWLEDGMENTS

PI Dr. Refai and his research team thankfully acknowledge Measurement Specialties for fabricating custom length piezoelectric sensor for project deployment. The company donated one Roadtrax BL (16'6) class 2 piezoelectric sensor for use in the single-element system and sixteen class 2 Roadtrax BL (1') piezoelectric sensors for use in the multi-element system. The sensors were essential to project success. The PI and his research team thank Mr. Daryl Johnson, Mr. Aaron Fridrich, and Mr. Brian Thompson at the Oklahoma Department of Transportation for facilitating highway deployments and developed system testing, as well as insightful conversations throughout the duration of the project. Last but not least, the PI thanks the Oklahoma Transportation Center for project funding.

ACCURATE VEHICLE CLASSIFICATION INCLUDING MOTORCYCLES USING PIEZOELECTRIC SENSORS

**Final Report
September 2013**

**Hazem Refai, Ph.D.
Principal Investigator
Williams Professor**

**Samer Rajab
Ahmad Othman
Omar Kalaa
Ahmad Mayeli
Graduate Research Assistants**

Oklahoma Transportation Center (OkTC)

201 ATRC Stillwater, Ok. 74078

TABLE OF CONTENTS

Executive Summary	1
Chapter I	3
Introduction.....	3
Proposed System.....	3
Organization.....	5
Chapter II	7
Background search.....	7
Related research work on vehicle classification	7
Chapter III.....	10
Systems design and preliminary testing.....	10
Single-element design and preliminary testing	11
Multi-element design and preliminary testing	15
Chapter IV.....	22
Validation systems	22
ADR system	22
Video validation system.....	23
Chapter V	25
Single element system development and highway testing	25
Algorithms	25
Data acquisition module.....	26
Socket server and initial processing module.....	28
Feature extraction and classification module.....	30
Track width over length classification method	33
Highway Deployments and Results	34
Highway deployment at AVC47	34
Highway deployment at AVC18.....	35
Highway deployment at AVC10.....	36
Highway deployment at AVC19.....	37
Principal component analysis.....	39
Vehicle classification using PCA and Bays networks including W/L ratio.....	41
Errors reported when processing Single-element data.....	43
Chapter VI.....	51
Multi element system development and highway testing	51
Algorithms	51

Pulse extraction.....	51
Feature extraction.....	52
Vehicle classification.....	53
Highway deployments and results	54
Effects of changing angle on the system.....	61
Differences between single element and multi-element classification systems.....	62
Errors reported when processing multi-element data.....	62
Conclusion	63
Implantation/Technology transfer.....	64
References.....	65
Appendix A	67
Appendix B	70
Appendix C	71

LIST OF FIGURES

Chapter I

Figure 1.1. Typical Weigh in Motion (WIM) System: two inductive loops and two piezoelectric sensors	3
Figure 1.2. Diagonal Placement of a Piezoelectric Sensor on a Roadway	4
Figure 1.3. Motorcycle Classification and Pulse Signature	4
Figure 1.4. Passenger Vehicle Classification and Pulse Signature	5
Figure 1.5. Four Axle Truck Classification and Pulse Signature	5

Chapter III

Figure 3.1. NI-9215 data acquisition unit	10
Figure 3.2. NI-9205 data acquisition unit	11
Figure 3.3. Single element vehicle classification system overview	11
Figure 3.4. Example of piezo-sensor expected output when triggered by a passenger vehicle	12
Figure 3.5. Aligned vehicle signals acquired by diagonal single element piezoelectric sensor a) car at 20mph b) car at 30mph	13
Figure 3.6. Time durations between 1st and 2nd tires and 1st and 3rd tires	14
Figure 3.7. Time durations of 1st and 2nd tires pulses.	14
Figure 3.8. Multi-element vehicle classification system overview	15
Figure 3.9. First round on campus testing deployment	16
Figure 3.10. Output signal from class 2 vehicle for first on campus testing deployment	16
Figure 3.11. Second round on campus testing deployment	17
Figure 3.12. Output signal from class 2 vehicle for second on campus testing deployment	18
Figure 3.13. Schematic of interface between sensor and DAQ	19
Figure 3.14. Aligned signal for class 2 using 12-element piezo sensor	20

Chapter IV

Figure 4.1. Schematic of ADR automatic vehicle classifier	23
Figure 4.2. VVT Flow Chart	24

Chapter V

Figure 5.1. Overall software architecture	25
Figure 5.2. Data acquisition phase	27
Figure 5.3. Socket client phase	28
Figure 5.4. Socket server and initial processing module	29
Figure 5.5. Feature extraction phase	31
Figure 5.6. Class 5 data	34
Figure 5.7. AVC18 deployment site schematic	36
Figure 5.8. Percentage of variance of data for PCs	40
Figure 5.9. Class 2 original signal and reconstructed signal	41
Figure 5.10. Pulse number vs. W/L ratio	42
Figure 5.11. Picture of class 2 vehicle missed by the sensor of Frame 16641	44
Figure 5.12. Example of a vehicle signal missed by sensor	45
Figure 5.13. Frame 42593	46
Figure 5.14. Saved Image before Frame 42593	46
Figure 5.15. Pulses from Frames 42418 through 43486	47

Figure 5.16. Frame 13303	48
Figure 5.17. Saved Image before Frame 13303	49
Figure 5.18. Saved Image before Frame 13303	49
Figure 5.19 Pulses from Frames 12857 through 14071	50

Chapter IV

Figure 6.1. Pulse extraction module.....	52
Figure 6.2. Feature extraction module	53
Figure 6.3. AVC19 deployment site and sensor layout	55
Figure 6.4. Raw signal from 15 aligned elements for class 2 vehicle.....	55
Figure 6-5. Speed distribution comparison between multi-element system and ADR for testing intervals 1 through 6	59

Figure A. 1. Helios computing system.....	67
Figure A. 2. DAQ I/O connector.....	68

Figure C. 1. Vehicle per vehicle reported output.....	71
---	----

LIST OF TABLES

Chapter V

Table 5.1. Diamond Traffic thresholds that were used in the developed classification algorithm	32
Table 5.2. Classification results by REECE compared to ground truth and ADR at AVC47	35
Table 5.3. Classification results for AVC 10	36
Table 5.4. W/L thresholds used for vehicle classification for AVC10 deployment	37
Table 5.5. Classification results for AVC 10	37
Table 5.6. (W/L) thresholds used for vehicle classification for AVC10 deployment.....	38
Table 5.7. Number of each class in data set.....	39
Table 5.8. Classification results using PCA and bays network on single element piezo-sensor	43
Table 5.9. Example of missed vehicle within vehicles from Frames 15376 through 17012	44
Table 5.10. Vehicles from Frames 42418 through 43486.....	47
Table 5.11. Vehicles from Frames 12857 through 14071.....	50

Chapter VI

Table 6.1. Thresholds used in multi-element classification algorithm	54
Table 6.2. Classification accuracy for AVC19 with 5kS/s testing round	60
Table 6.3. Classification accuracy for AVC19 with 10kS/s testing round	61
Table 6.4. Comparison between single element and multi-element systems.....	62

Executive Summary

The Federal Highway Administration (FHWA) evaluates fatality rates and estimates trends based on travel data measurements. Miles of travel per vehicle classification (VMT) is reported to the FHWA to determine risk exposure for vehicle collision. It is critical for the FHWA to receive accurate data measurements. However, a report published in September 2008 (Reassessment 2010+) prepared by the Highway Performance Monitoring System (HPMS) indicated the quality of reported travel data for motorcycles is questionable. The inability and inconsistency of current traffic monitoring equipment to detect and classify motorcycles is an urgent problem.

This report presents research, hardware, and the development of a software algorithm for a computer-based system to count and classify vehicles, in particular motorcycles. The system uses piezoelectric sensor(s) embedded in roadways to detect traveling vehicles regardless of shape, size, or weight, and then categorize them according to 13 FHWA-published vehicle classifications. The system design differs from current piezo-based classifiers in two primary aspects: 1) Unlike the current perpendicular configuration, the piezo-sensor is positioned diagonal to traffic flow, and 2) The piezo-sensor is segmented into a number of individually addressable elements with the potential to estimate vehicle width and velocity (in addition to performing vehicle classification).

The system is comprised of a piezoelectric sensor(s), analog-to-digital converter, and an embedded computer that performs digital signal conditioning and classification processing algorithms. The configuration was developed to accommodate either a single or multi-element piezoelectric sensor embedded diagonal to traffic flow and to provide comprehensive vehicle detection between road shoulders. When a vehicle travels over the sensor, a force is applied to the sensor surface, generating an electrical charge from the activated piezoelectric sensor. An analog-to-digital converter translates the charge into voltage at an amplitude proportional to the applied force. In this way a vehicle with four wheels generates four distinct pulses, e.g., one pulse per wheel. A motorcycle with two wheels generates two pulses. Hence, vehicles with different classifications and number of axels, sizes, and shapes are characterized by a unique train of pulses that distinguishes them from one another. Since several different piezoelectric sensors are activated for each vehicle wheel, the distance between activated sensors and the time difference between the two activations can be determined, and, in turn, axel spacing, vehicle width track, and velocity can be obtained. A computer is required to acquire and analyze sensor pulses to determine vehicle classification and velocity, and then communicate real-time information to a database housed in an ODOT server.

The developed system was able to achieve upwards of 84.4% classification accuracy using a single element piezoelectric sensor with generic average width; a range of 94.8% and 99.07% accuracy with (Width/Length) ratio using custom thresholds; and 86.9% accuracy using multi-element piezoelectric sensors. Overall impact of the system includes classification accuracy for motorcycles at tremendous cost savings when compared to current equipment and maintenance system costs. An added benefit is the prospect of relaying real-time traffic volume and average speed on Oklahoma highways and roadways to ODOT personnel.

This Page Is Intentionally Blank

Chapter I

Introduction

A current and widely adopted industry solution for vehicle classification combines one or two strips of piezoelectric sensors and/or inductive loop detectors [1-2], as shown in figure 1.1. An inductive loop detects a vehicle by measuring changes in magnetic field responding to vehicle metal. The signal from a piezoelectric sensor detects an axel by measuring force from axel weight; having a vehicle trigger two sensors indicates total number of axles and facilitates a calculation of vehicle speed and inter-axle distance. These factors can then be used to classify the vehicle. To execute this method of classification, two full-lane or half-lane piezoelectric sensors are installed on the roadway at a preset distance from one another. Figure 1.1 illustrates a system using loop-piezo-loop-piezo configuration.

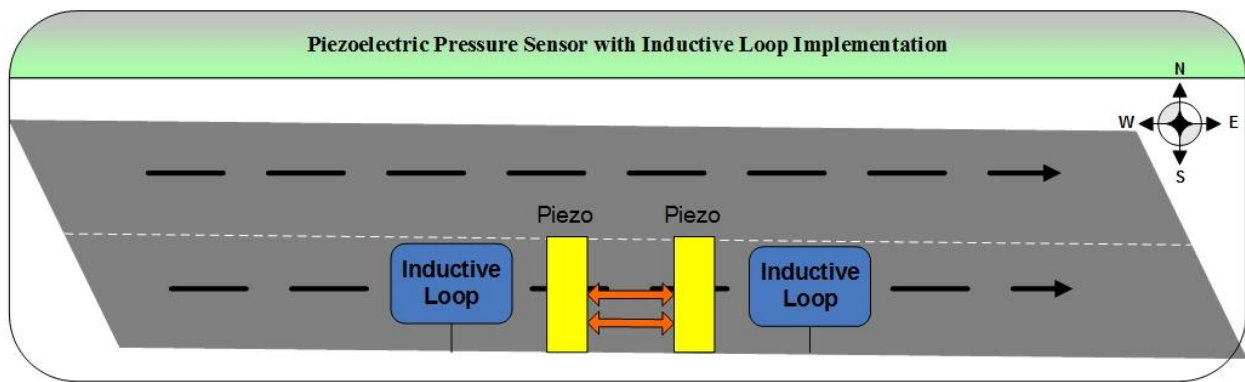


Figure 1.1. Typical Weigh in Motion (WIM) System: two inductive loops and two piezoelectric sensors

This type of system has a number of advantages, including the ability to identify the class of the passing vehicle, as well as its speed and weight. However, one significant problem of this configuration is the high rate of inaccuracy in motorcycle classification. Regrettably, when the unit is calibrated to weigh heavy trucks, it becomes impervious to motorcycle weight. Additionally, motorcycles pale in size when compared to most vehicles, making it highly likely that motorcycles could avoid traveling across loops, thus avert detection. Furthermore, many motorcycles are built with a limited amount of metal, which hampers detection even when one travels directly across the loop. We propose a modified version of sensor configuration that mitigates possible misclassification of motorcycles. An added benefit of this system is cost savings—by utilizing a single- or multi-element piezoelectric sensor placed diagonal to traffic flow in an unconventional way, sensor length (thus total product quantity) is reduced.

Proposed System

The project proposes using piezoelectric technology—similar to that used in the weight in motion (WIM) system—to accurately detect and classify vehicles into 13 vehicle types, including motorcycles. The technology employs measurement of force instead of magnetic field to classify motorcycles traveling on highways and roadways. This method effectively eliminates detection failure due to a limited amount of metal in the motorcycles. When a motorcycle or vehicle travels over the piezoelectric sensor, an electrical charge/discharge signal of amplitude proportional to the weight of the traveling vehicle is generated.

The sensor employed in the proposed design consists of an array of piezoelectric sensors and is placed diagonally, instead of perpendicularly, to traffic flow on the roadway, as is typical of current WIM installations. As such, the sensor covers the roadway from shoulder to shoulder. Figure 1.2 illustrates the diagonal placement of the piezoelectric sensor. Given this configuration, a vehicle with four wheels will generate four distinct pulses: one pulse per wheel. A motorcycle with two wheels will generate two distinguishing pulses. In this way, vehicles with different classification, number of axels, size, or shape will be characterized by a unique train of pulses different from others. Figures 1.3 to 1.5 shows the unique train of pulses for a motorcycle, a passenger vehicle, and a truck.

The figures illustrate that the piezoelectric sensor is multi-element, comprised of several sensors that can be uniquely identified by channel or multiplexer. An approaching vehicle activates one (or two) sensor element(s) depending on the number of wheels overpassing them. Hence, distance between activated sensor elements can be determined, and, in turn, car width can be calculated, e.g., distance between a vehicle's wheels. Vehicle velocity can then be calculated using car width and the measured time difference between the first and second signal pulses. The unique advantage of this system is that it facilitates measurements of tire number and vehicle width. Additionally, axel spacing and vehicle velocity can be measured with two inductive loops and a piezoelectric sensor, providing two additional measurements necessary for accurate motorcycle detection and classification.

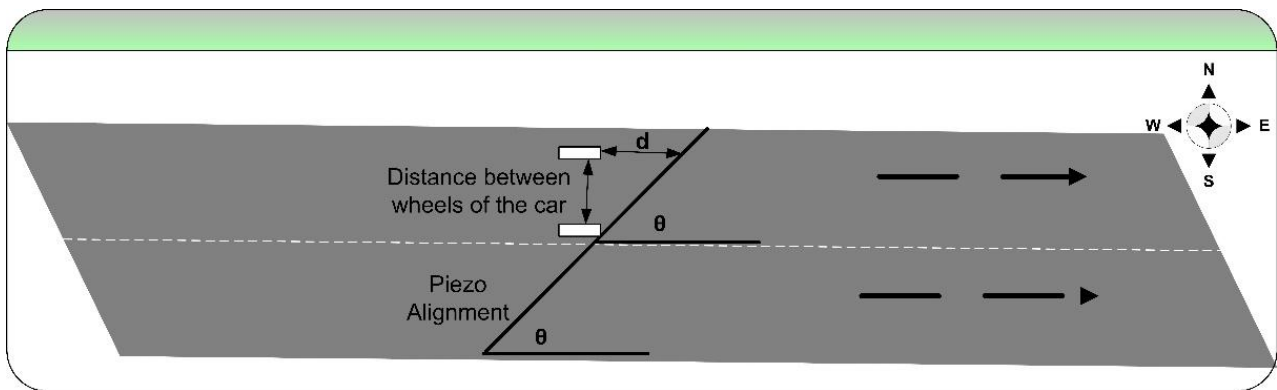


Figure 1.2. Diagonal Placement of a Piezoelectric Sensor on a Roadway

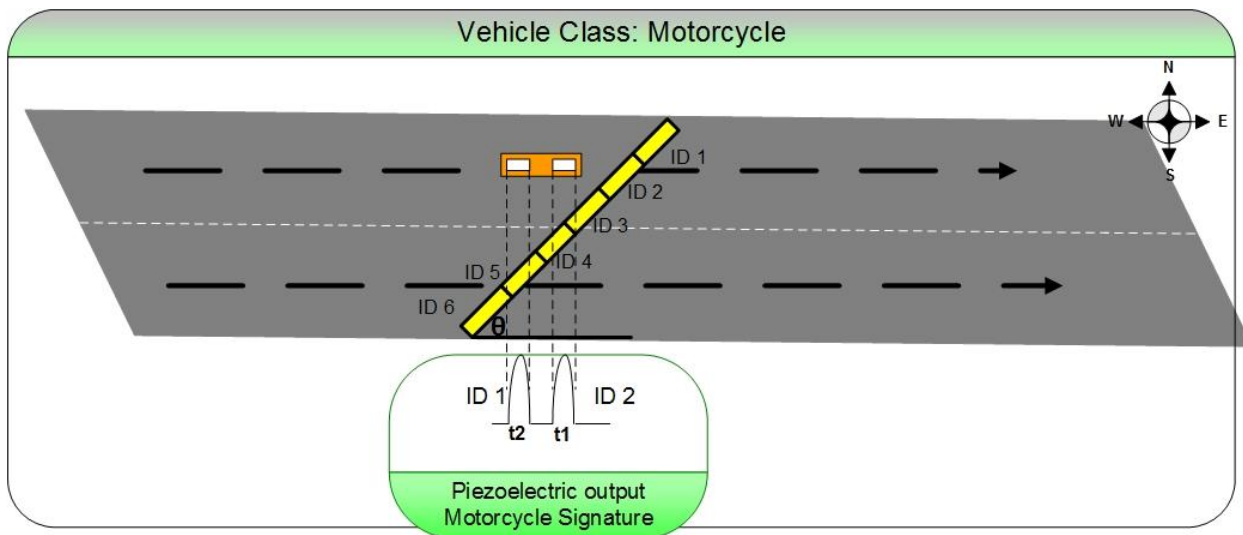


Figure 1.3. Motorcycle Classification and Pulse Signature

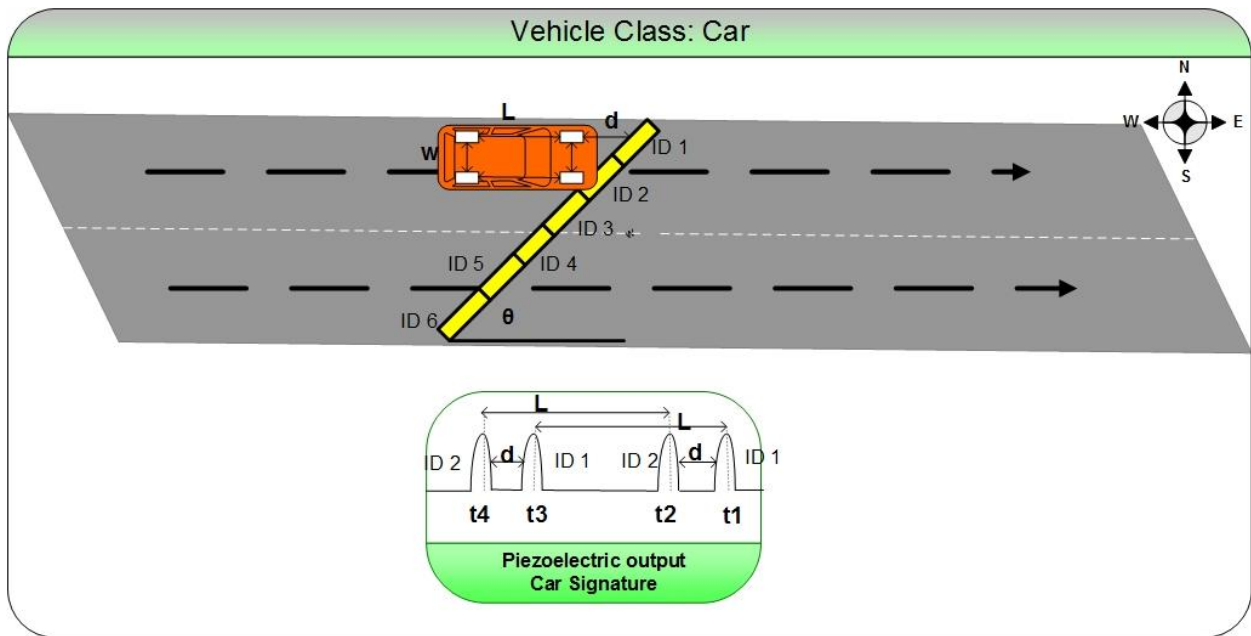


Figure 1.4. Passenger Vehicle Classification and Pulse Signature

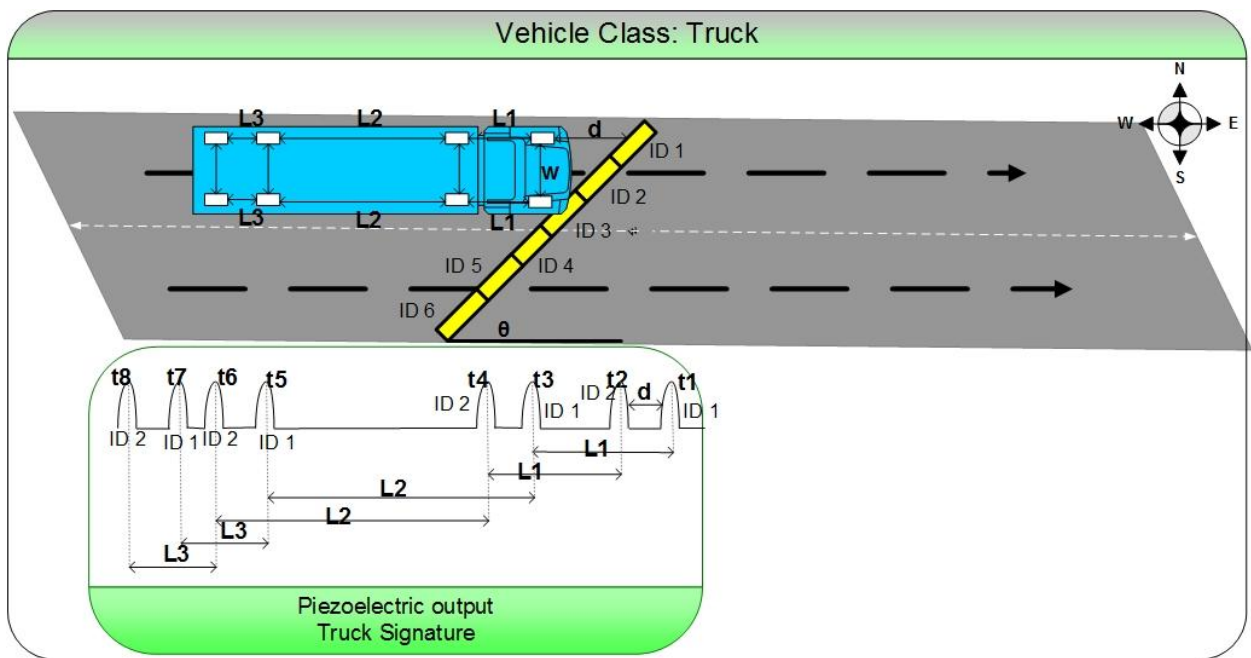


Figure 1.5. Four Axle Truck Classification and Pulse Signature

Organization

This report is organized as follows. Chapter II highlights background literature. Related vehicle classification, single inductive loop classification, and speed determination, as well as various classification algorithms, are also described. Chapter III details single- and multi-element piezo-based

system development and on-campus preliminary system evaluation. Chapter IV provides a brief description of the two ground-truth systems used to validate classifier accuracy, and Chapter V presents classification algorithms, including a novel scheme developed for the single-element sensor design. Results of system field-testing in realistic highway deployment are also discussed in Chapter V. The multi-element sensor design is explained in Chapter VI, and highway deployment classification results are presented in Chapter VI. The report concludes and future work is suggested in Chapter VII.

Chapter II

Background search

Vehicle sensing devices have been investigated for over 40 years and reported in both research and industry literature. FHWA and DOTs are typically interested in the most up-to-date methods and results.

In this section several classification schemes are detailed according to methodology.

Related research work on vehicle classification

Keawkamnerd et al. [3] utilized two Anisotropic Magneto-Resistive (AMR) sensors placed on a mounted 8x8 roadside board with sensors located next to each other. The board was located at roadside to collect signals from passing vehicles. From vehicle data researchers extracted a hill pattern of the magnetic signal, energy level, and magnetic length. This setup measured the number of signal peaks generated by from an inductive loop. A moving average was computed for the time series of the received signal to reduce sampling rate. The differential magnitude, along with the new energy-level moving averages, were computed to obtain the amount of energy change—rise or fall—during vehicle detection. Minimum, maximum, and normalized energy levels were computed based on vehicle speed and sampling period. These parameters were combined in a decision algorithm to classify four types of vehicles, namely motorcycle, car, van, and pickup. An overall classification accuracy of 81.69% was achieved.

Sokra studied data fusion techniques using parameters collected from an inductive loop and a piezoelectric sensor [4]. The magnetic profile of the inductive loop includes mean value, mean square value, standard deviation, maximum value, moment of third order, and central moment of third order. These factors, along with the others like vehicle length, speed, and number of axles, were used in membership functions based on fuzzy logic. Classification accuracy ranged from 68 to 92% for triangular membership function and from 68 to 94% for Gaussian membership function. An overall performance improvement was noted for the Gaussian membership function.

Sun et al. investigated a vehicle classification system comprised of two inductive loops and an Inductive Classifying Artificial Network (ICAN) [5]. ICAN is a self-organized feature map (SOFM) that uses inductive loop output to perform classification for a number of classes, e.g., similar to the number of neurons. The test set consisted of 300 selected vehicles of which four categories were chosen for testing. Classification rate accuracy was 81%. However, when a more complicated scheme with nine categories was employed, classification rate accuracy decreased to 71%. Limiting classification to seven categories for two separate data sets reached accuracy levels of 87% and 82%.

Gajda et al. investigated the impact of loop length on vehicle classification in [6]. Loop lengths in the range of 0.25m to 4m with a step of 0.25m were tested, as was a separate 10cm loop used for reference. Signals acquired from inductive loops were normalized for velocity and sampling frequency. Several signal characteristics, mainly the magnetic profile, were used as criterion to define vehicle type. Test vehicles included two types of buses and a passenger vehicle. Testing demonstrated that shorter loops furnish more highly distinguished criterion, and, thus, improved differentiation between the three vehicle types. Also, vehicle axles were clearly distinguishable in the 10cm loop magnetic profile.

Gajda et al. researched the use of one inductive loop to calculate passing vehicle speed [7]. Researchers were able to obtain a correlating parameter between the inductive loop signal and vehicle speed independent of vehicle type. Passing vehicle speed was measured and comparisons were made between one- and two-loop systems. Given a 10m separation between inductive loops, the two-loop system demonstrated an inherent error occurring between the loops in response to vehicle acceleration or deceleration. Results indicated a velocity calculation with maximum RMS error of 2.5Kmph. The authors did not provide information on classification type or accuracy rate.

Wang and Nihan developed an algorithm that used a single inductive loop to estimate speed and classify vehicles accordingly [8]. The researchers assumed data contained two vehicle types: Short Vehicles (SVs) and Long Vehicles (LVs). SVs were assumed to have uniform length, which aided in speed estimation. The algorithm divided data collected from a single inductive loop into 20-second intervals in which some contained only SVs and others contained a mix of SVs and LVs. Intervals containing zero number of vehicles were removed. Next, data from a fixed, five-minute period that contained only SVs intervals was processed. Using Eq. (1), the algorithm estimated speed using SVs interval, and then applied it to all remaining intervals within the same five-minute period. Test runs were performed at four sites. Estimated error for speed and volume were compared to results obtained from a dual-loop system. The estimated mean error for speed was found near zero with a standard deviation of smaller than 6.2km/h. The estimated mean error for volume was insignificant, as well; however, the standard deviation ranged between 2.76 to 3.38, which is relatively large for a period of five minutes.

$$s_i = \frac{N(i)}{T.O_i \cdot g} \quad (2.1)$$

where:

N= Number of vehicles in interval;

i = interval time index;

s = space mean speed for interval;

O = duty cycle of loop; and

g = speed estimation parameter

Meta and Cinsdikici used a single inductive loop for vehicle classification [9]. Their system was comprised of a single loop with dimensions of 2m X 1m, an inductive loop detector, a validation camera, and a computer. Their contributions include signal preprocessing, data set reduction, and a method for choosing the proper training set for a neural network vehicle classification system. They chose a five-category classification scheme: car, van, truck, bus, and motorcycle. The novel approach employed principal component analysis (PCA) rather than down-sampling for processing and applicability to Neural Networks (NN).

PCA is a method that compresses data in an intelligent manner wherein vehicle data collected by the sensor in one domain (e.g., time) is transformed into another domain (e.g., frequency) only with significantly fewer data point representation. The components—or coefficients in the new domain—represent variance between data in the original domain and that in the new domain. The main component holds the highest variance between the two data sets. Any subsequent components hold variance values of less significance. Thus, by eventually using a limited number of components or features rather than the entire original data set, we can distinguish different vehicle types and perform classification. A more detailed description of PCA technique will be presented in Chapter 5. Meta and Cinsdikici used a number of principal components containing more than 99% variance between data observations in the data set.

A data set of 1,000 vehicles was used for training the neural network, and a data set of 1,330 vehicles was used for testing purposes. Overall classification accuracy was 94.21%.

This work can be compared to work completed during the project reported herein, e.g., a single sensor type was used to acquire traffic data along with PCA for feature extraction. The difference between the two lies in the fact that in our approach we use a single element piezoelectric sensor rather than an inductive loop. The advantage is accurate motorcycle detection using less complicated algorithms. In our

PCA feature extraction, we mined features for an eight (rather than five) category system with features covering less variance between data observations, i.e., approximately 92%, while achieving comparable classification results.

Zhang et al. used an electrical resistance strain gauge sensor based on piezoresistive material to detect vehicle axels [10]. Three in-pavement sensors were used, and each axle was found to produce its own peak on the output of each individual sensor. Vehicles were classified into five categories—small truck, medium truck, bus/large truck, 3-axle truck, or combination truck—using the Support Vector Classification (SVM) learning pattern recognition/classification technique. A data set of 602 vehicles was collected from highway traffic: 50% were used for training, 25% for validation, and 25% for testing. Classification accuracy was 96.4%.

Bajwa et al. developed a wireless sensor classification system using vibration and detection sensors [11] to indicate individual axles from pavement structure vibration. Although four accelerometers were implanted in the pavement, data from only three were used after one sensor failed to produce results. Two magnetometers were installed at a fixed distance from one other, and then used to calculate vehicle speed based on arrival time at each of two sensors. Fifty-three trucks were tested. Axle detection accuracy ranged from 86.8 to 90.6% when using a single sensor and approached 100% when using sensors in a deliberately combined manner. Notably, test results were used for axle detection, not vehicle classification.

Golla et al. simulated a design for vehicle type and tire width on a highway [12]. The system consisted of 16 or 49 polymer conductor segments to comprise a sensor. The segments undergo closure in the event of tire impact with a goal of distinguishing number of tires, and their width and type. Simulation was performed for sensor frequency response to determine physical dimensions. Only then is sensor able to detect tires at a maximum highway speed of 100mph. No experimental testing was provided.

Chapter III

Systems design and preliminary testing

This section describes the single- and a multi-element system and their designs. Also included are results from preliminary on-campus testing performed to ensure an appropriate signal is acquired from sensors and that signal preprocessing was executed properly. Preliminary testing is vital to advance the project, as it lays the groundwork for final highway deployment. Both single- and multi-element systems must be evaluated under typical highway conditions to validate system capability for collecting accurate signals and achieving appropriate classification. Prior to highway deployment, however, connection to DAQ and signal integrity should be investigated. This was accomplished for both systems by way of a series of lab and on-campus road tests for both systems.

Initially an interface to the computing device had to be developed to relay the signal from sensors. Two DAQs were used for development and testing:

1.) **NI-9215** DAQ has four inputs, as shown in Figure 3.1. This configuration enables simultaneous sampling rate up to 100KS/s on the four well-isolated analog inputs. Resolution is 16bit, and maximum voltage range is -10v to 10v with maximum accuracy of 0.003v



Figure 3.1. NI-9215 data acquisition unit

2.) **NI-9205** DAQ has 32 single ended (SE) or 16 differential inputs, as shown in Figure 3.2. The configuration enables a maximum of 250KS/s sampling rate divided among a number of active input channels. Resolution is 16bit, and maximum voltage range is -10v to 10v with a maximum accuracy of 6220 μ v.



Figure 3.2. NI-9205 data acquisition unit

Single-element design and preliminary testing

The single-element vehicle classification system is comprised of one piezoelectric sensor, a DAQ, and the embedded computing system, as shown in Figure 3.3. Although the single-element design was not included in the original OTC proposal, PI Dr. Refai and his research team investigated this design due to its uncomplicated, single-channel DAQ implementation.

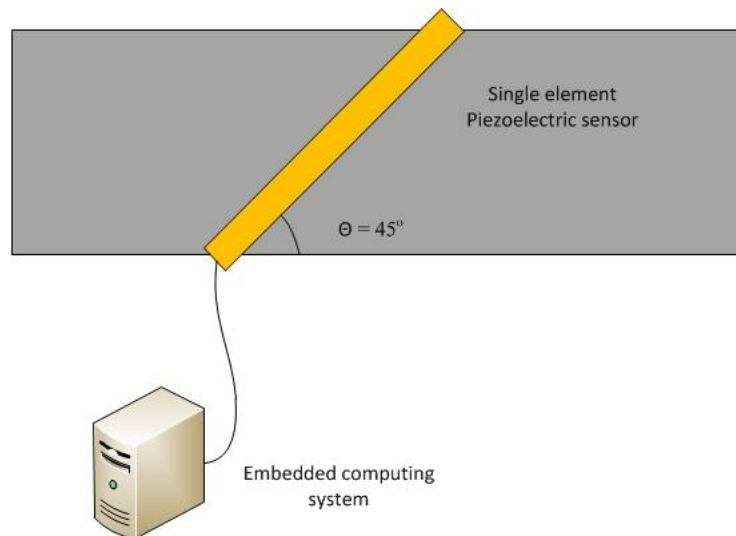


Figure 3.3. Single element vehicle classification system overview

It is mandatory that the sensor cover the entire traffic lane diagonally across a lane of traffic at a certain known degree, ensuring that each tire of a passing vehicle produced an output pulse. As such, length constraints must be met. Roadtrax BL manufactured by Measurement Specialties was selected primarily because the sensor was specifically designed as a traffic sensor and maintains suitable signal integrity for our application. These signals were analyzed through a feature extraction algorithm where pulses from each passing vehicle were detected so that vehicle-related parameters could be computed.

Data was subsequently sent to the classification phase of the algorithm. In this way, motorcycle class 1 vehicles were accurately classified, primarily because they are the only class characterized by two tires, resulting in two pulses. For the remaining 13 FHWA classes, vehicle velocity was required to distinguish among classes with the same number of tires. Tire and axle spacing were required to set thresholds

between different classes with the same number of tires and axles. In turn, vehicle track width—defined as the distance between two tires on same axle—was needed to calculate vehicle velocity and achieve classification. Figure 3.4 illustrates an example of piezo-sensor expected output when triggered by a passenger vehicle

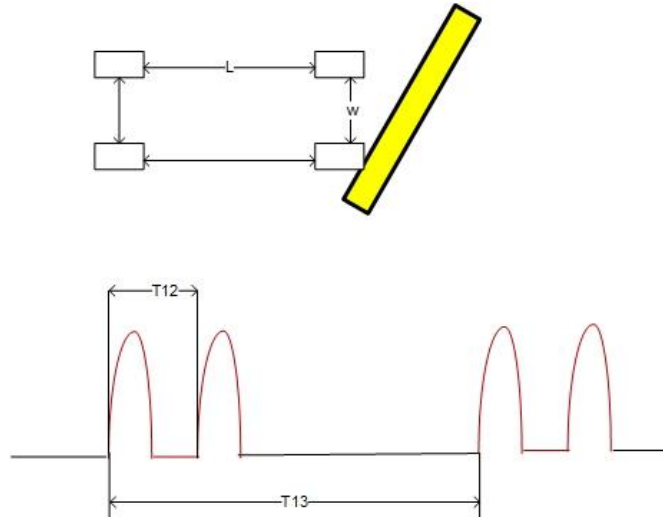


Figure 3.4. Example of piezo-sensor expected output when triggered by a passenger vehicle

Using vehicle track width w , velocity V , and axle spacing L can be determined using the following equations:

$$V = [w * \cot(\theta)] / T12 \quad (3.1)$$

$$L = V * T13 \quad (3.2)$$

Notably, given a single-element design, the system is unable to measure or provide vehicle track width. Figure 3.4 indicates that each tire impacting the piezoelectric sensor generates a signal pulse, even though the location of the impact cannot be determined because sensor consists of only a single element. A segmented or multi-element design was developed to mitigate this limitation.

Preliminary Campus Testing Results

This subsection offers on-campus test results that highlight the effects of changing velocity and vehicle type over output signal.

Figure 3.5 shows examples of aligned test runs for a passenger car. In graph (a) four aligned runs are plotted to represent test results in which a driver was asked to maintain a speed of 20mph. Graph (b) plots four aligned runs depicting results when the driver was requested to maintain a speed of 30mph. A comparison is beneficial for highlighting uniform output at the same velocity for the same vehicle. Notably, uniformity will be disturbed when either velocity or axle spacing changes. Both parameters affect the time between pulses and the shape of detected signal pulses, consequently affecting vehicle classification. Figure 3.5 demonstrates that as velocity increases both amplitude level and time duration of the signal pulse decreases. Also, in (a) we can see that slight changes in vehicle velocity have a clear

impact on output signal. Variations in velocity are effects of the driver failing to maintain a constant speed for all test runs.

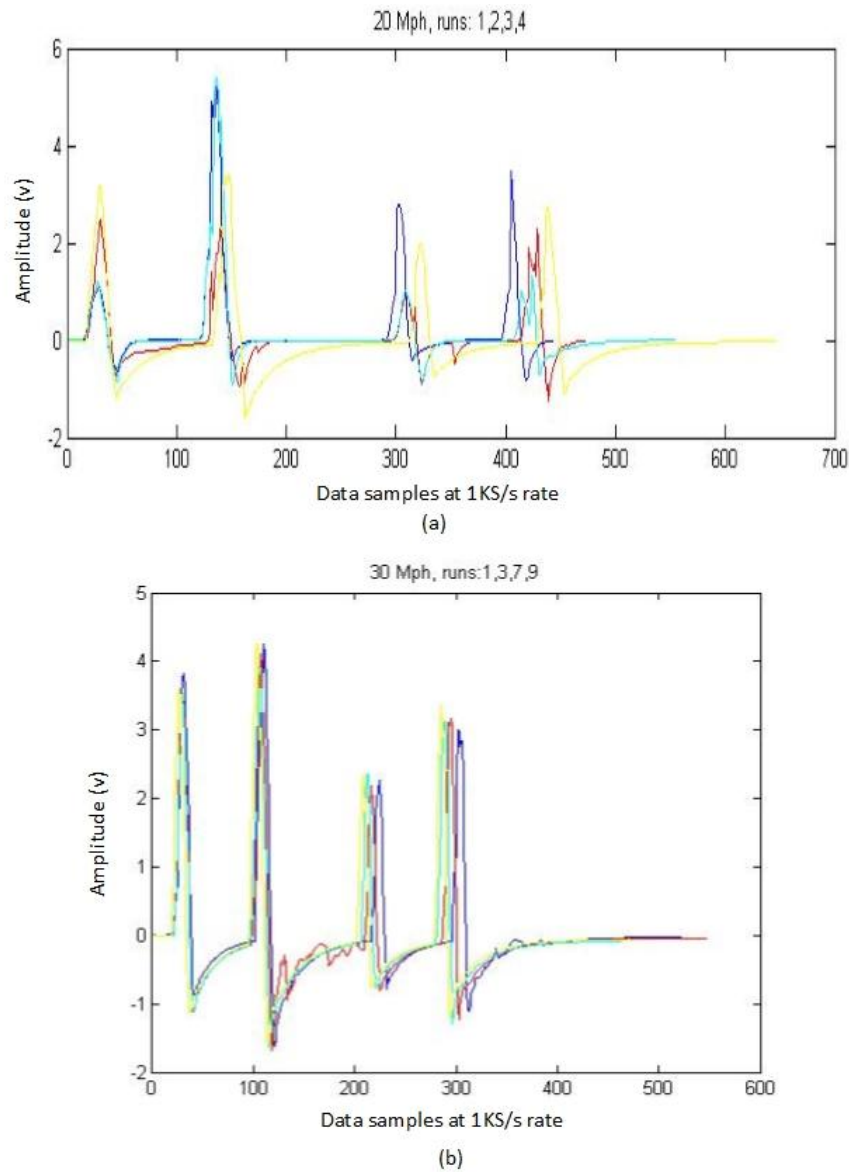


Figure 3.5. Aligned vehicle signals acquired by diagonal single element piezoelectric sensor a) car at 20mph b) car at 30mph

A test set of 11 runs for a passenger car vehicle was used to monitor changes in inter-pulse periods at various velocities that ranged between 15 and 30 mph. Figure 3.6 plots time durations between the first and second pulse and between the first and third pulse. Duration between the first and second pulse corresponds to vehicle track width; duration between the first and third pulse corresponds to vehicle axle spacing.

In Figure 3.7, time duration of the first pulse and second pulse are plotted against test vehicle velocity, which ranged between 15 and 30mph, as shown in Figure 3.6. Results in Figures 3.6 and 3.7 aided in determining an appropriate sampling rate for the embedded system DAQ unit. As vehicle velocity

increases, the time interval between individual pulses decreases, requiring an increase in sampling rate to accommodate for the higher frequency signal. Variation in inter-pulse time also has a direct effect on detected axle spacing due to a change in velocity.

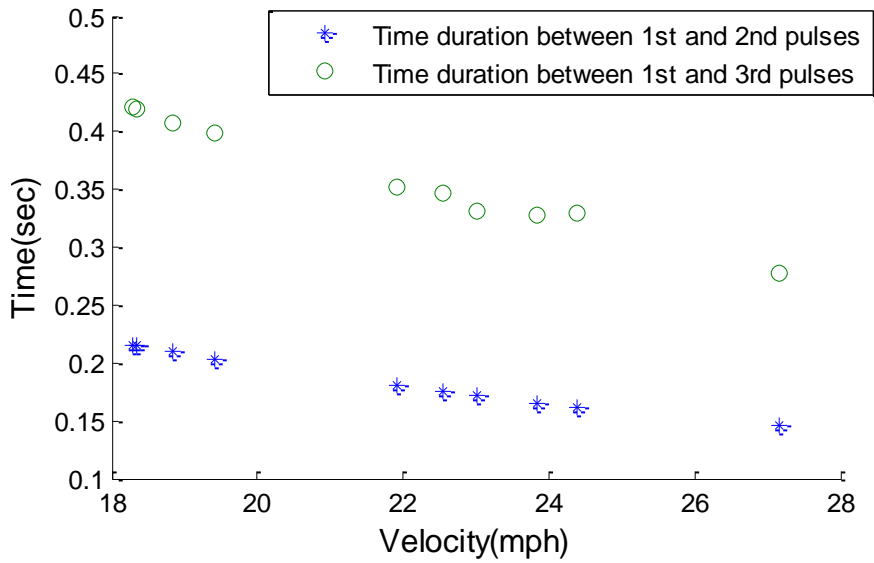


Figure 3.6. Time durations between 1st and 2nd tires and 1st and 3rd tires

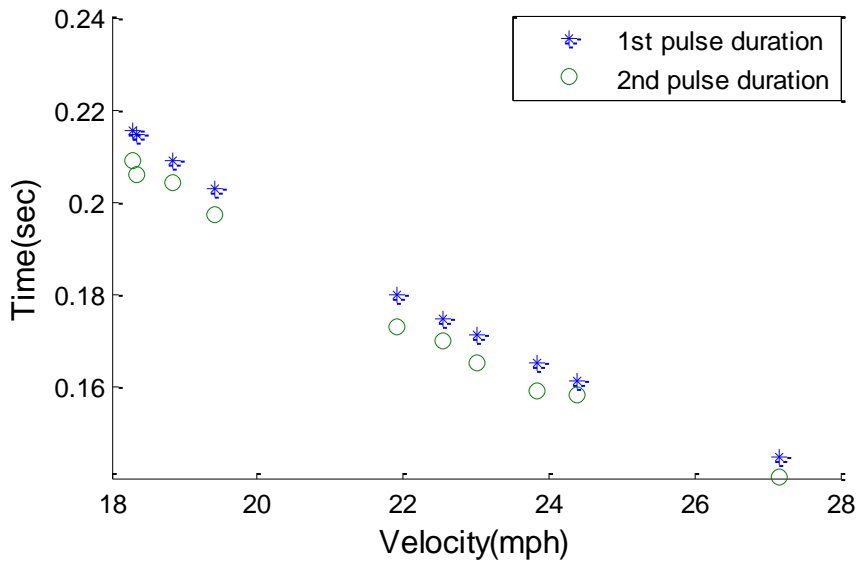


Figure 3.7. Time durations of 1st and 2nd tires pulses.

Multi-element design and preliminary testing

Unlike single-element design, the multi-element sensor (constructed with several piezoelectric sensors) is able to estimate the distance between two tires on the same axle, thus determine vehicle track width. Using Eq. (3.1) and Eq. (3.2), the classification algorithm calculates speed and axel spacing, respectively.

The basic design consists of 16 piezoelectric sensor elements—each 1.5ft long, including sensor, as well as the hard casing that connects the sensor to its coax wire. Piezoelectric sensor elements are arranged successively and installed into a pocket road tape. It is necessary that the tape remain affixed on the road at a specified angle (θ). Wires connecting sensor elements are channeled to the roadside DAQ via a second protective pocket road tube placed parallel to the one housing the sensor elements, as shown In Figures 3.8 and 3.9.

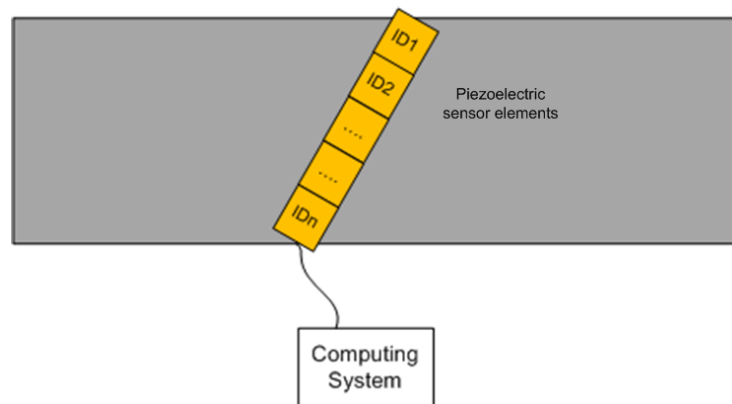


Figure 3. 8. Multi-element vehicle classification system overview

Preliminary Campus Testing Results

Preliminary testing included lab and on-campus road evaluation. The purpose of lab testing is to properly interface sensor elements to DAQ and ensure sensor output signal integrity. Labview signal express was used to collect and store data.

Following lab testing, several on-campus road tests were performed. The latter was crucial to the success of highway deployment. A range of issues (from problems with sensor element road installation to signal coupling between various DAQ channels) arose during on-campus deployment. Solutions were proposed and implemented to minimize highway deployment errors.

Three on-campus road tests with multi-element sensor were performed, as noted below:

1) Four-element testing with NI-9205

The purpose of this deployment was to test sensor signal output when impacted with a vehicle tire. Figure 3.9 shows the diagonal deployment of the four elements. During testing a high level of crosstalk among the DAQ channels was observed. Crosstalk makes it difficult to accurately distinguish impacted elements (channels) from those non-impacted although indicating a signal. See Figure 3.10, in which a signal appears on all four channels, in spite of the fact that vehicle impact was

only detected on the element connected to channels 1 and 2. Peak amplitude of noise detected on the non-impacted channel was 30 to 40% of that detected on the impacted channel (channel 2 in our case). The cause for crosstalk between channels is the result of impedance mismatch between piezoelectric sensors and DAQ input channels. This issue is discussed in more detail later in this chapter.



Figure 3.9. First round on campus testing deployment

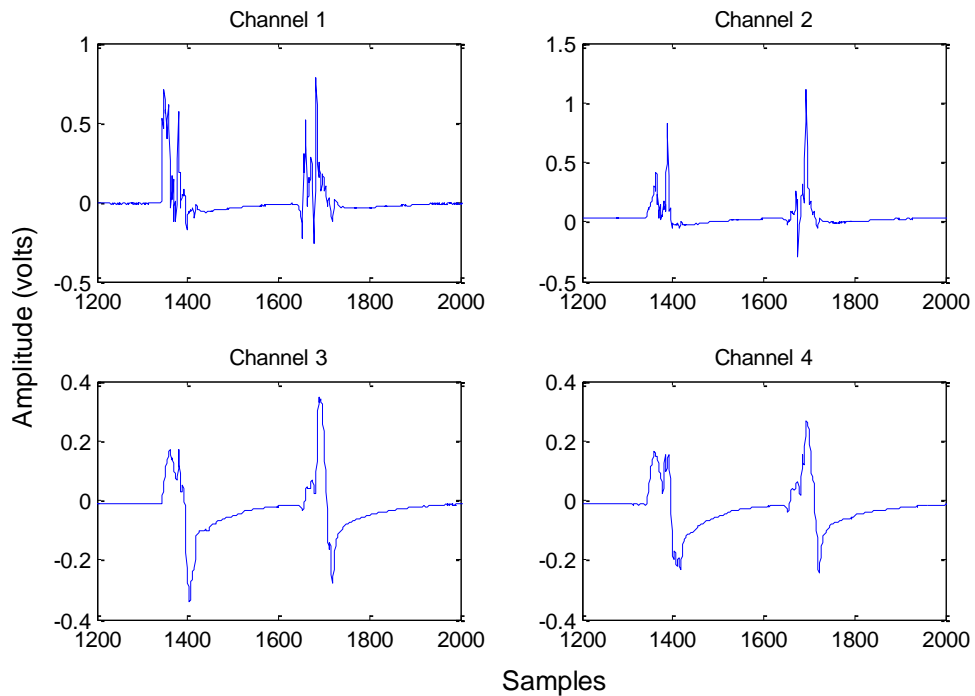


Figure 3.10. Output signal from class 2 vehicle for first on campus testing deployment

2) Four-element testing with NI-9215

To overcome the crosstalk problem, a test with NI-9215 DAQ was performed. Unlike NI-9205 used in the previous test runs, DAQ NI-9215 has analog-to-digital (ADC) channels that are isolated from one another, thus minimizing crosstalk among them. The four-element piezoelectric sensor was placed on a traffic lane similarly to the setup shown in Figure 3.11. Results of this deployment indicated a noticeable signal quality improvement and the essential reduction of crosstalk among channels, as shown in Figure 3.12. However, this solution is expensive, especially given the 16-element sensor design planned for highway testing deployment.



Figure 3.11. Second round on campus testing deployment

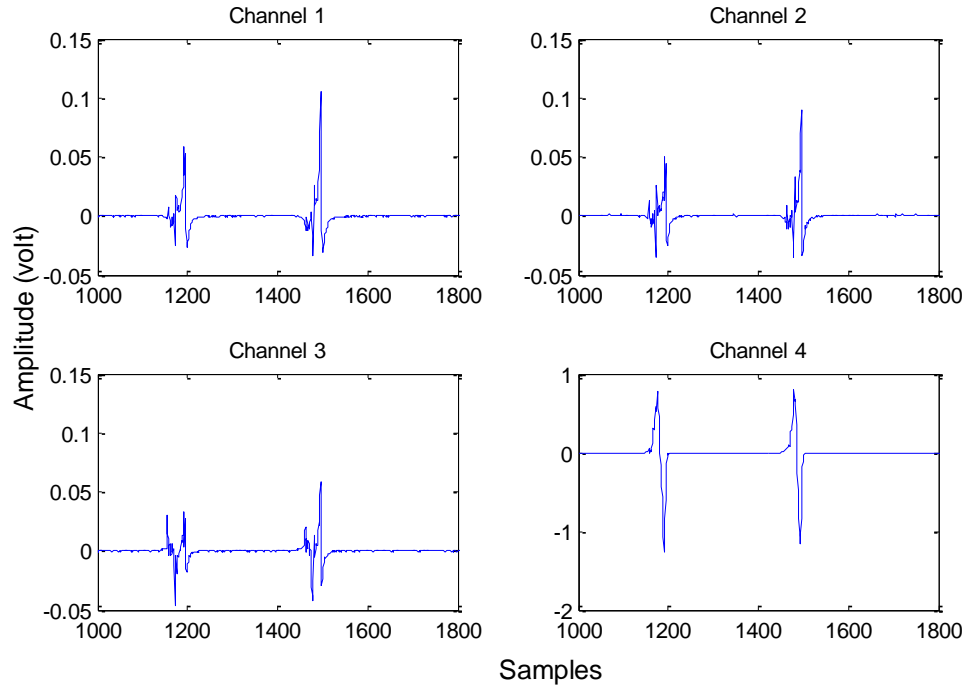


Figure 3.12. Output signal from class 2 vehicle for second on campus testing deployment

Coupling and crosstalk among channels was further investigated to provide more stable readings from the sensor while taking advantage of the inexpensive multi-channel NI-9205 DAQ with multiplexer. The piezoelectric sensor proved to have high impedance once connected to the DAQ, thus preventing the discharge of the DAQ single internal amplifier. As such, when the DAQ multiplexer advanced to the adjacent channel to measure its applied voltage, the remaining capacitor charge interfered with current voltage measurement and resulted in crosstalk and erroneous readings. Several solutions were proposed: 1) Reduce piezoelectric sensor impedance using operational amplifiers with high input impedance and low output impedance; 2) Reduce sampling rate to provide the DAQ amplifier capacitor additional time to discharge its previous measurement; and 3) Apply differential signal acquisition. The third solution was adapted due to minimal implementation costs, which in turn lead to the development of the interface used in highway deployment. Figure 3.13 details the interface design.

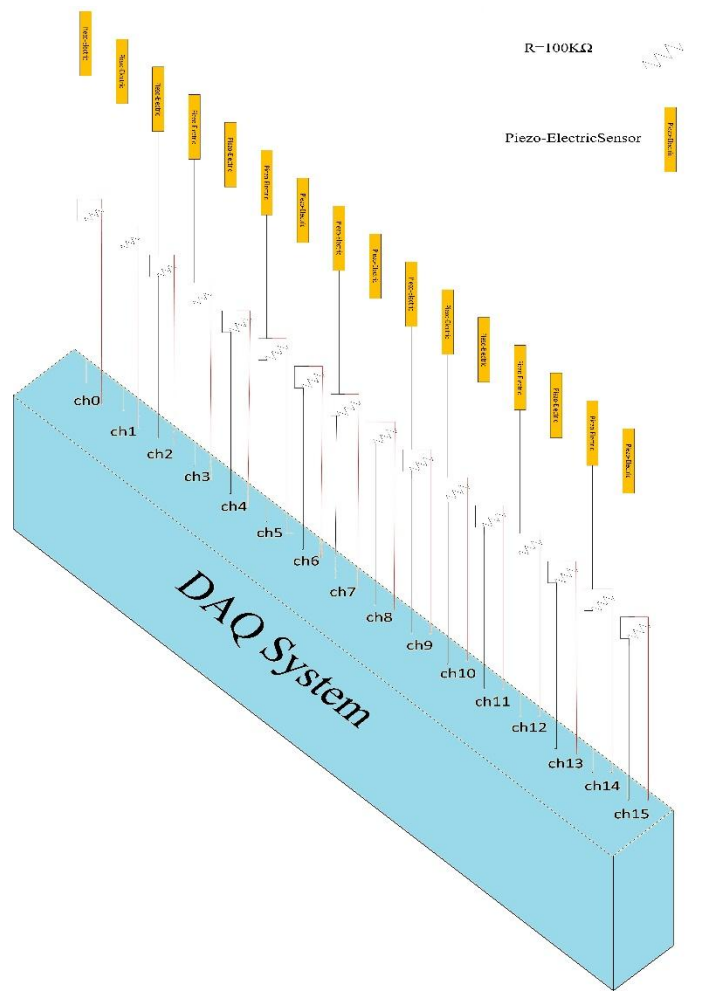


Figure 3. 13. Schematic of interface between sensor and DAQ

3) Twelve-element testing with differential NI-9205

The sensor layout in the NI-9205 DAQ test setup was similar to the two previous campus deployments shown in Figures 3.9 and 3.11. Again, three vehicle types, namely a car, van, and truck, were tested. The vehicle driver was requested to travel at various predetermined speeds. Test results from the third deployment carried out with the differential solution showed tremendous improvement over the initial deployment. Signals from various sensors were distinguished by limited crosstalk. Figure 3.14 shows signals captured from a passenger vehicle as it passed over all 12-element sensors.

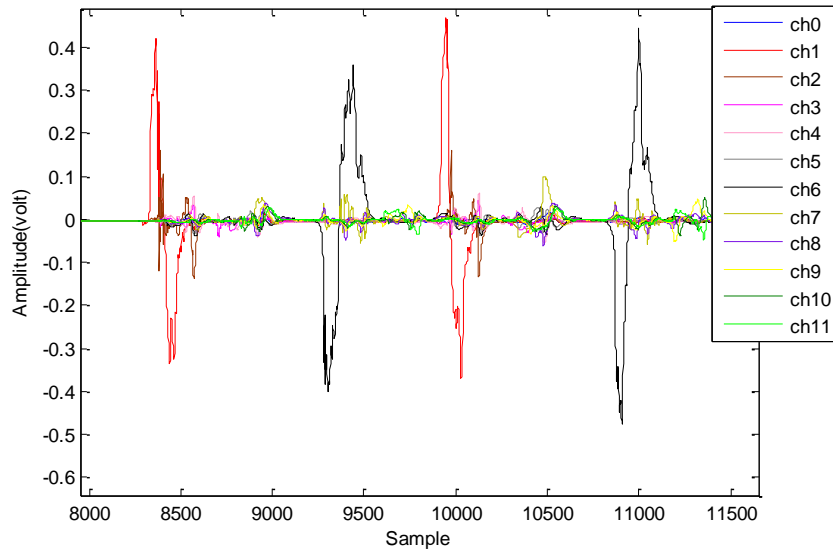


Figure 3.14. Aligned signal for class 2 using 12-element piezo sensor

Data acquired via various test runs were processed accordingly, including extraction and timing of pulses, as well as impact element identification. Speed was also calculated using extracted features, and then compared with monitored speed enforced by the driver. Table 3.1 provides the speed results of the on-campus 12-element filed-testing deployment.

Table 3.1. Speed analysis for third on campus testing deployment

test	car type	Approximate speed (mph)	Calculated Speed
1	car	10	10.865
2	car	10	10.8912
3	car	10	10.1971
4	car	20	19.3569
5	car	20	19.1519
6	car	20	18.3174
7	car	30	28.6974
8	car	30	29.3486
9	car	30	28.205
10	Van	10	8.2254
11	Van	10	7.5394
12	Van	10	8.4208
13	Van	20	18.8327
14	Van	20	16.8181
15	Van	20	17.9716
16	Van	30	28.9657
17	Van	30	27.1871
18	Van	30	27.6374

Chapter IV

Validation systems

Developing a functional vehicle classification system that accurately detects motorcycles is the primary goal of this project. To render the project successful, the system must be validated after all system components, including hardware and software, are complete. Highway testing facilitates vehicle data collection required for classification. Ground-truth data is also required for comparison. This chapter highlights two validation systems employed during the project:

1. ADR classifier—an Automatic Vehicle Classifier (AVC)—already deployed by Oklahoma Department of Transportation (ODOT) on highways.
2. Video camera validation system—developed by the University of Oklahoma research team.

ADR system

Over 70 AVC sites are dispersed on highways throughout the state of Oklahoma. ODOT utilizes these to collect vehicle volume, speed, and classification, and then uses the data to design future Oklahoma roadways, bearing in mind road capacity and pavement endurance.

The OU research team tested the developed classification systems within close proximity to permanent ODOT AVC sites that have been equipped with Peek Traffic manufactured ADR controllers. Each test site was comprised of two inductive loops with a piezoelectric sensor situated between them. The array of sensors was connected to an ADR to analyze the signal and provide classification data. Speed can be calculated from dual loop data since the distance between the two loops is predetermined. Axle number and spacing is calculated with the use of the piezoelectric sensor. Data is used to calculate vehicle speed and compare classification.

ADR traffic data includes the number of vehicles per class within each speed bin recorded during a programmed time interval. The minimum recording time possible with ADR is one minute. Vehicle speed is binned every 5mph, starting at 30mph and ending at 80mph. Tables containing number of vehicles in each class per speed bin is generated within a mere 60 seconds of data collection. See Figure 4.1 for a schematic of ADR automatic vehicle classifier

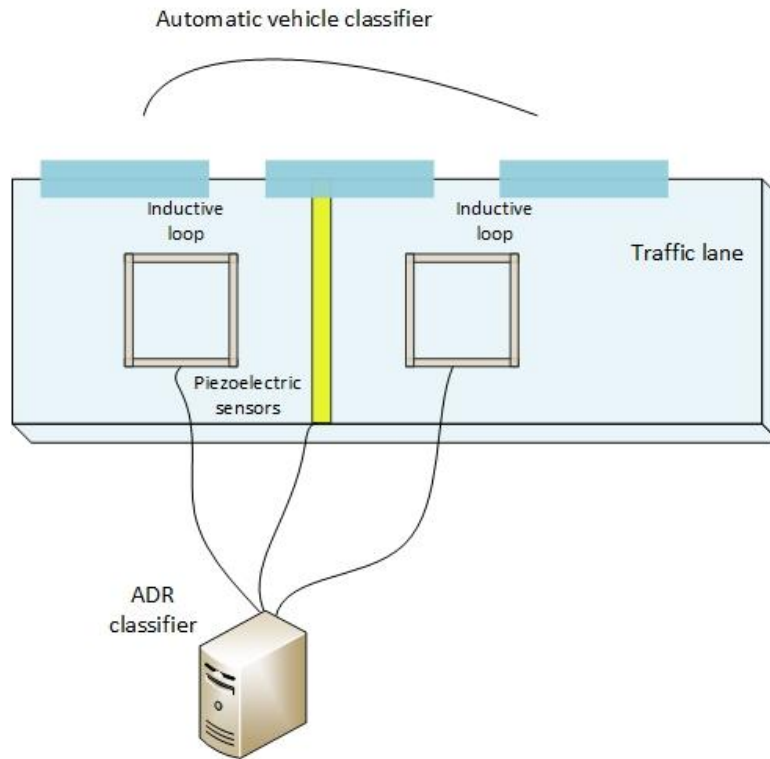


Figure 4.1. Schematic of ADR automatic vehicle classifier

Video validation system

A video recording ground-truth system was employed to validate the newly developed system. The PI and his research team initially began recording video images of passing vehicles traveling on a highway situated within close proximity of a predetermined deployment site. Video footage was scheduled for a given time period once the camera became synchronized with the single- or multi-element sensor-based system. Video recorded during initial tests was analyzed manually, pausing on each passing vehicle image to record class, lane, and video time parameters. This manual process proved extremely taxing and time consuming. As such, researchers were motivated to write a software program to automate processing and logging tasks. The program user was still tasked with determining class and lane parameters.

A flow chart of the newly developed Video Validation Tool (VVT) is provided in Figure 4.2: VVT flow chart. The algorithm starts by initializing video object then creating output files to save data into. Detection mask dimensions are set to require vehicle detection. Motion detection commences when the frame displays motion. User then sets vehicle class among other information, which will be saved to a file. If no motion is detected, the algorithm continues scanning frames until the last frame of the video is reached.

VVT utilizes the *initial input* of video files taken from two video cameras strategically placed in order to monitor traffic from two complementing point of views:

- 1) An image from the highway to detect a vehicle's motion when it crosses a predefined mask area.
- 2) An image from video recorded on the highway to provide an added level of certainty when determining a vehicle's class.

VVT requests *user input* for the flow of information following the detection of each vehicle class, traveling lane, frame number or time of detection, as well as top and side vehicle image.

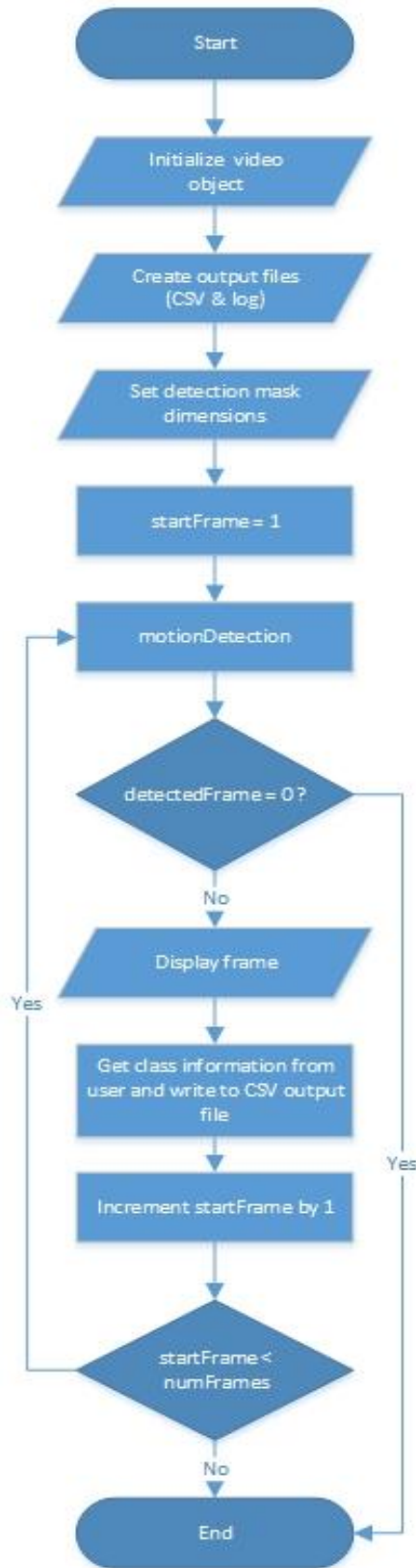


Figure 4.2. VVT Flow Chart

Chapter V

Single element system development and highway testing

This chapter describes algorithms developed for the single-element vehicle classification system and also reports on algorithm testing during highway deployment.

New algorithms were developed using both Matlab and C in order to implement data acquisition, data processing and feature extraction of acquired signals, and vehicle classification. Highway deployment evaluated overall system performance and compared the newly developed single-element sensor results with those obtained from the ADR ground-truth system and video recordings.

Algorithms

This section provides a detailed description of program architecture developed for the project. System architecture can be defined as the path taken from the commencement of raw data acquisition by DAQ to the decision stage of the algorithm's classification phase. The vehicle classification algorithm can be separated into two phases: feature extraction and classification.

Program development was implemented for ODOT Roadside Embedded Extensible Computing Equipment (REECE) using C. C is widely accepted as the programming language of choice for embedded systems. It has flexible structure with various functions. Figure 5.1 illustrates the overall software architecture. The program is comprised of three primary modules: data acquisition; socket server and initial processing; and feature extraction and classification.

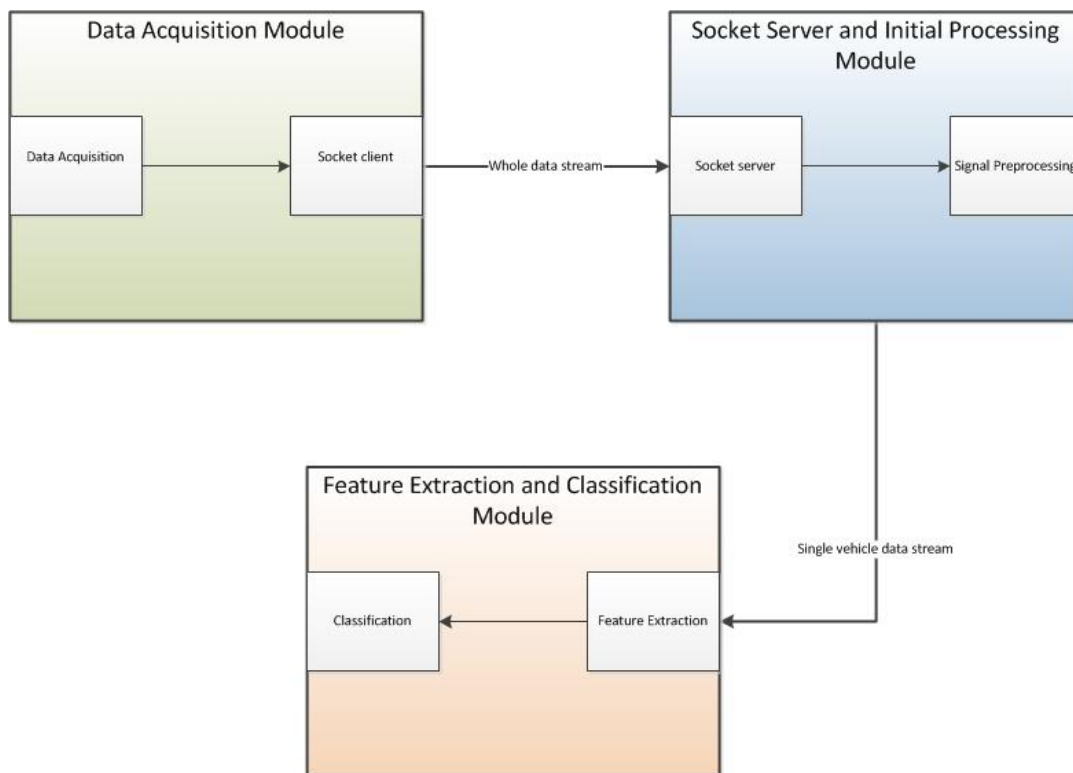


Figure 5. 1. Overall software architecture

Data acquisition module

The data acquisition module of the program encompasses the actual data acquisition phase and a socket client phase. This module configures the DAQ, collects raw data, formats it in character form, and then uses a Linux socket to send it to the data processing module. Two phases and their tasks are highlighted below:

- Data acquisition phase: This phase (or sub-module) is responsible for raw data collection. The REECE DAQ is used for piezoelectric sensor output sampling. The program includes initiating the board, configuring the sampling parameters, and ensuring data is not lost due to slow processing. The phase flow graph and details are depicted in Figure 5.2. The process commences by initializing and configuring the DAQ. It scans sensor output and, then goes into sleep mode for short amount of time before reading the buffer. This is required so that the buffer is not empty. The algorithm wakes up, and then scans the buffer. If the number of new samples is greater than 10, the algorithm reads the samples from the buffer in a cyclic fashion. If fewer than 10, it continues in sleep mode. If samples are overwritten before reading, an error (e.g., not processing fast enough) is reported.

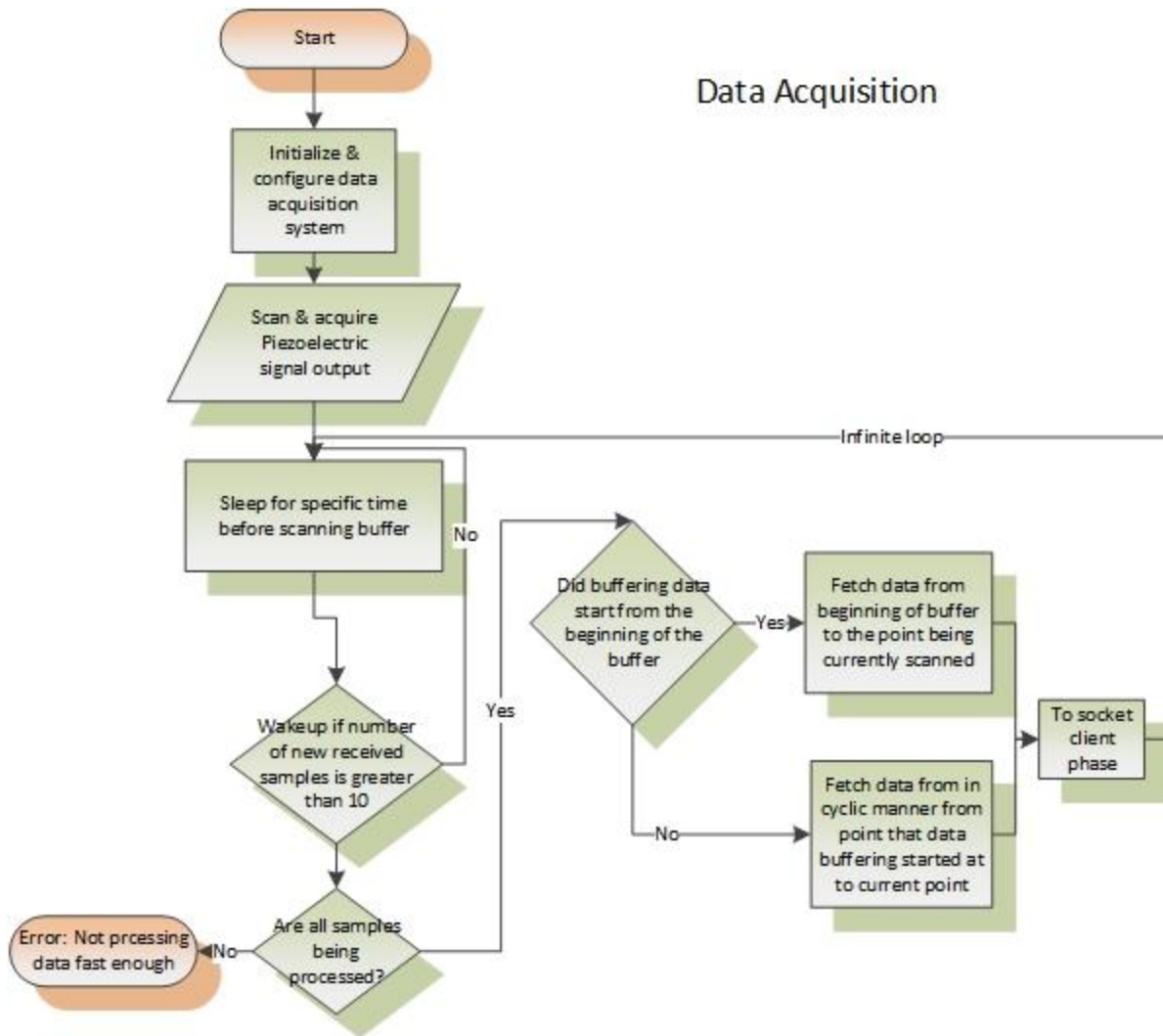


Figure 5.2. Data acquisition phase

- Socket client: Socket sends raw data from the DAQ module to the socket server and initial processing module. By using a multiple process scheme, the Linux multi-tasking/threading property is leveraged so that the data processing load can be distributed among different processes. In this way uninterrupted data acquisition is ensured. During the data acquisition phase, data is fetched from the DAQ buffer on a regular basis. Notably, if all data processing relied on the same data acquisition process without multi-threading, latency and data loss could result.

Sockets are the most widely used method for inter-process communication in Linux-based operating systems. The client side of the server sends data in character form. Stream socket was selected for this project to guarantee sequenced, reliable data exchange. Stream socket uses Transmission Control Protocol (TCP), which is a reliable sequenced data transmission protocol. See Figure 5.3 for socket client phase detail. In this phase raw data is received and modeled as a character stream. A socket connection opens to a server process and sends data to it.

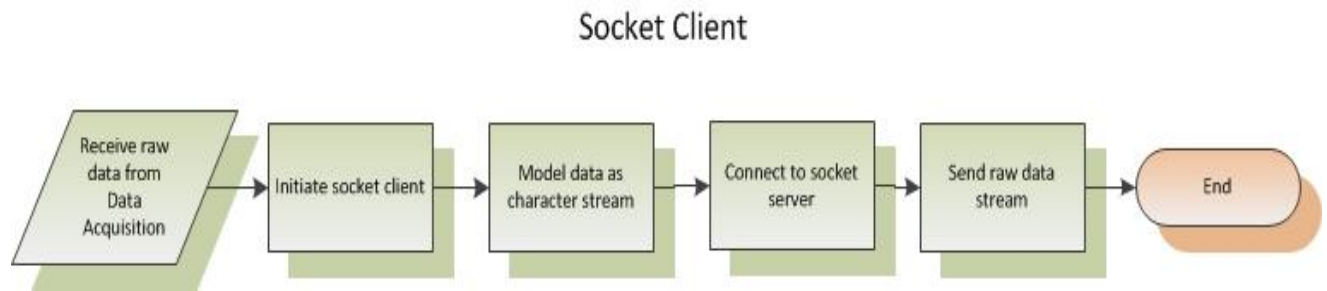


Figure 5.3. Socket client phase

Socket server and initial processing module

The socket server and initial processing module is responsible for a number of tasks, including receiving raw data from the socket client, initial data processing, and utilizing the multi-threading, call-feature extraction, and classification module. Vehicle data is a function input.

The socket server first listens for a connection with the client. After client connection and commencement of data streaming, the socket server continuously receives data and converts it from character form to floating point for processing feasibility. The purpose for initial processing is to isolate single- or multiple-vehicle data so it can be sent to the feature extraction and classification algorithm for further processing. Consequently, zeros are suppressed from occupying system resources.

As raw data is received from the socket client, the socket server tests sample values. Given that they pass a certain negative or positive threshold, the detection flag is raised and samples are stored as vehicle data. If a predetermined number of zeros equal to two seconds is surpassed, vehicle detection ceases and stored vehicle data is provided to the feature extraction and classification module as input. Figure 5.4 illustrates a flow graph of the socket server and initial processing module. This phase commences by listening to connection from client and then receiving data stream from socket server. It models character stream into raw data, and then begins to detect vehicles. Given no detection, the algorithm performs calibration every three minutes. Given a vehicle is detected, then algorithm begins saving the signal and calculating time duration, where continuous zero amplitude values in the signal occur. If this duration passes a certain value, then data for a vehicle is considered already acquired. Algorithm passes this data to feature extraction phase on a separate thread.

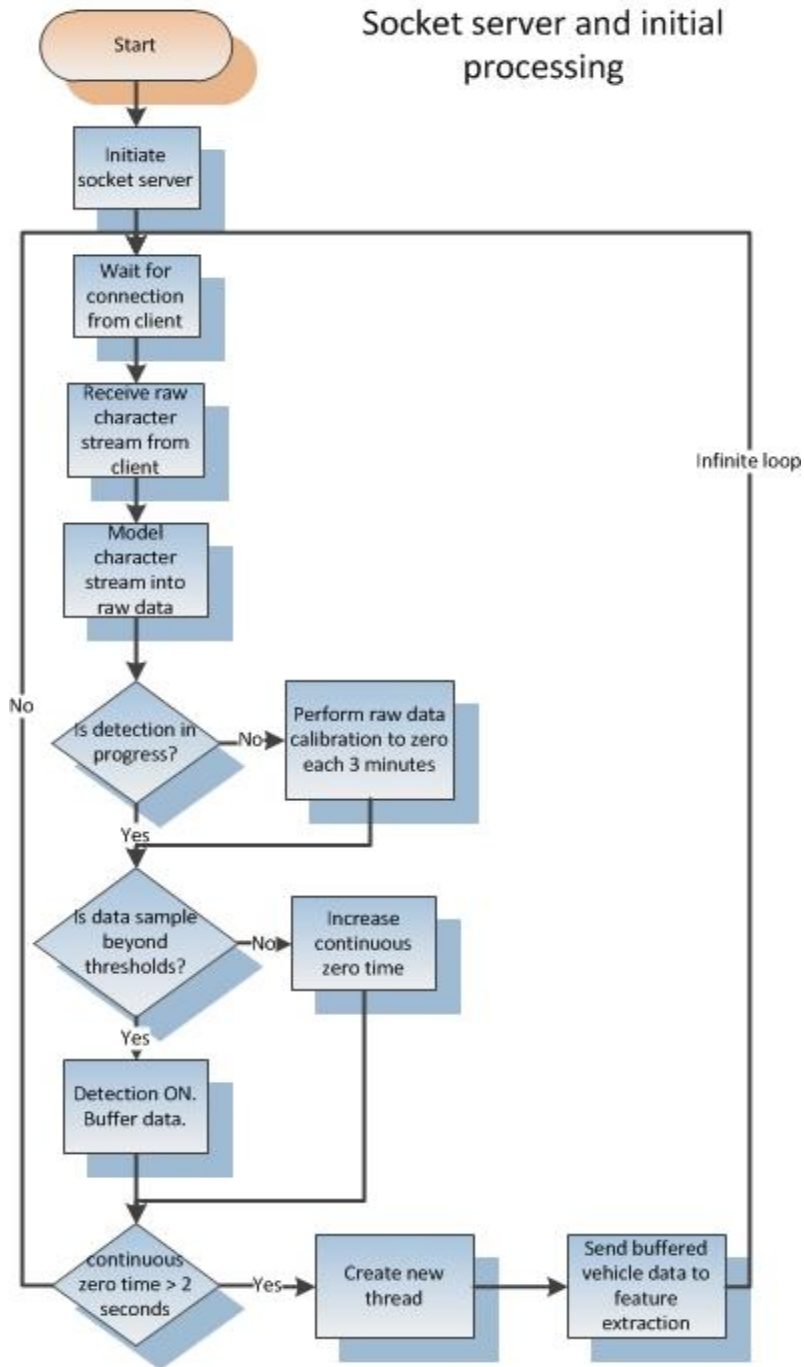


Figure 5.4. Socket server and initial processing module

Feature extraction and classification module

The feature extraction and classification module represents the vehicle classification algorithm. This algorithm constitutes the logic used to process raw data into useful information, including the parameter and class of passing vehicles. Feature extraction and classification modules are carried out on a separate thread to take advantage of operating system multitasking. Hence, the father process can return to raw data processing while the child process performs feature extraction and classification. The thread takes function to be executed and pointer to some data as input. Feature extraction function, isolated vehicle data, and number of samples in isolated vehicle data are passed to a new thread.

The feature extraction phase is responsible for passing vehicle detection and subsequent extraction of characterizing information and specifications for classification purposes. After acquiring and preprocessing a piezoelectric response signal associated with one passing vehicle, pulses associated with distinct vehicle tires are identified and total number of vehicle tires is disclosed. Likewise, time at which each pulse commences is detected, which indicates intermittent time difference between pulses. The extracted vehicle information is used to determine vehicle velocity, tire/axle spacing, and total number of tires. Results will then advance to the classification phase.

Regular sensor output calibration is added to the code to solve signal bias resulting from temperature and pavement effects, among other variables. During calibration the mean of sensor output signal is calculated regularly and removed from received raw data. Figure 5.5 illustrates the details of the feature extraction phase. The process commences by initializing a new thread and receiving vehicle data from socket server module. Pulse detection subsequently begins. When the first two pulses are detected, algorithm calculates vehicle speed using average speed. The algorithm continues with pulse detection until a maximum axle spacing of 35 feet is surpassed, indicating that vehicle data collection is complete. Finally, algorithm calculates number of tires and axle spacing, and then sends the information to classification phase.

Feature extraction phase

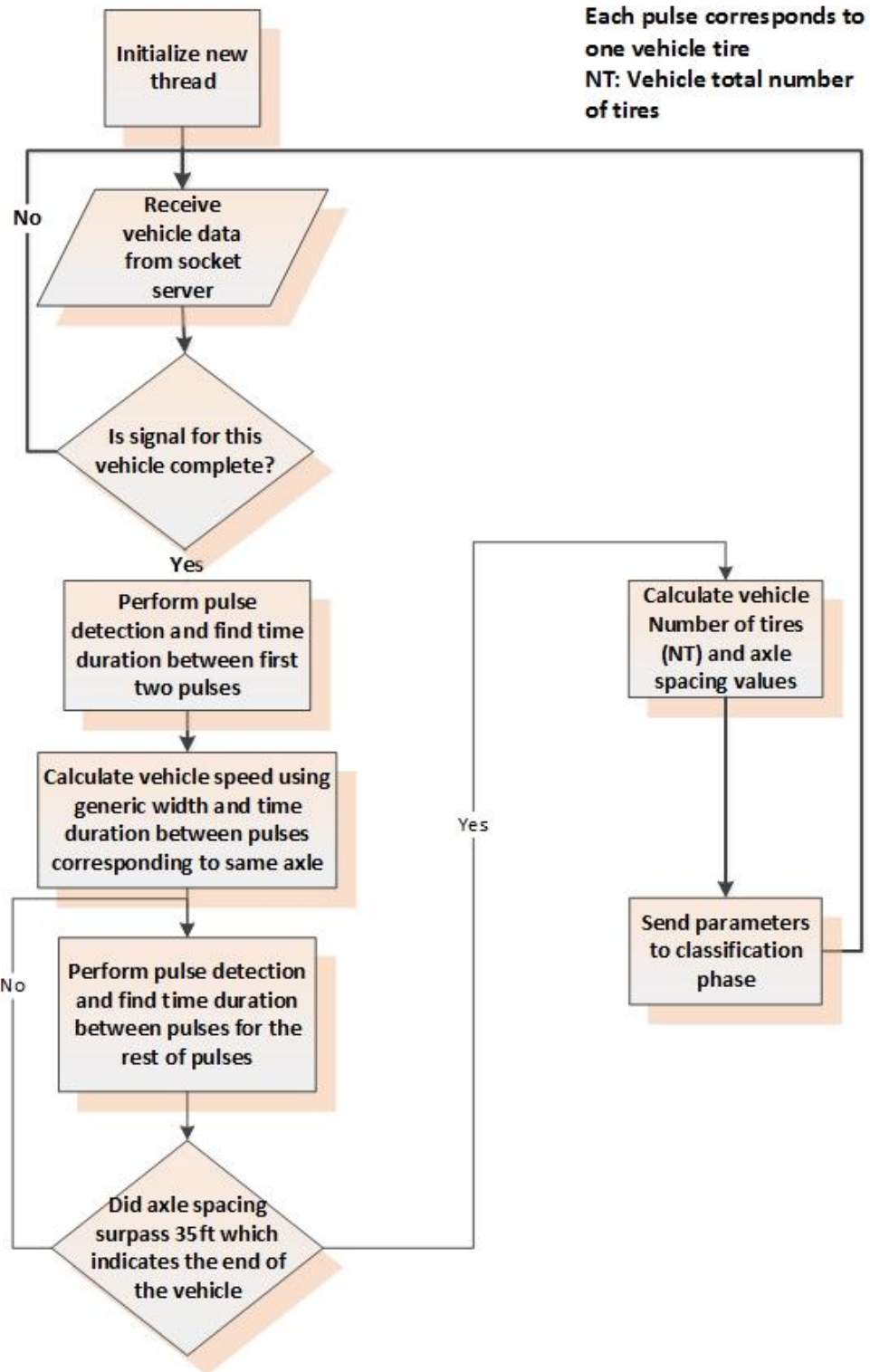


Figure 5.5. Feature extraction phase

Classification phase

The classification phase categorizes vehicles into 13 FHWA classes using vehicle information acquired and calculated in the feature extraction phase. Required parameters include number of tires, axle spacing for various axles, and time of pulses triggered by tire number relative to class.

Accurate motorcycle classification is accomplished by counting the number of tires impacting the sensor element. However, classification for other vehicle classes is not possible if only number-of-tires is used because differentiating between vehicle classes is limited due to overlapping parameters. As such, a number of standard classification thresholds and algorithms were investigated. Thresholds developed and published by Diamond Traffic were eventually implemented. This algorithm utilizes passing vehicle axle spacing to produce a classification decision.

A report by Diamond Traffic suggests axle spacing bins be used for vehicle classification. However, classification was ultimately based on the use of two straight piezoelectric sensors rather than a single, diagonally positioned sensor. Thus, the developed algorithm uses suggested axle spacing only after tire count data eliminates motorcycles from analysis. Axle spacing can then be determined by tire/pulse spacing. Thresholds were applied to yield a classification decision. Table 5.1 presents the exploited thresholds.

The developed classification algorithm is also designed to filter an amount of erroneous or incomplete sensor activation. For example, let's consider an event of 12 pulses, i.e., 6 axles. Depending on axle/tire spacing values, a certain vehicles might not always be classified as class 10 or class 12. Hence, if axle spacing values don't satisfy thresholds for either class, the event is considered a false trigger. This phenomenon is particularly useful to minimize false detection, e.g., vehicle combining.

Table 5.1. Diamond Traffic thresholds that were used in the developed classification algorithm

Bin	Axles	Axle spacing (an "*" corresponds to any calculated value)
1	2-3	1-5.8, *
2	2-3	5.9-10.2, 10-18.8
3	2-3	10.3-15, 10-18.8
5	2	15.1-24
4	2-3	23.5-99.9, *
8	3	*, 18.1-99.9
6	3	*, 3.5-8
2	4-5	1-10.2, *, 1-3.4, 1-3.4
3	4-5	10.3-15, *, 1-3.4, 1-3.4
8	4	*, 5.1-99.9, 3.5-99.9
8	4	*, 1-5, 10-99.9
7	4	*, *, *
11	5	*, 6.1-99.9, *, *
9	5	*, 1-6, *, 3.5-11
3	5	9.9-15, *, *, 1-3.4
5	5	15.1-24, *, *, 1-3.4
9	5	*, *, *, *
10	6	*, 3.5-8, 3.5-8, *, 8.1-99.9
12	6	*, *, *, *, 8.1-99.9
10	6-10	*, *, *, *, 3.5-8, 3.5-8, 3.5-8, 3.5-8, 3.5-8

Track width over length classification method

Specific vehicle classification requires gathering distinguishing signal characteristics. These are extracted from the signal, and then used to perform classification. Signals vary upon the sensor employed to monitor vehicles, e.g., piezoelectric, magnetic field, vision, or inductive, among others.

Our approach utilized a single-element piezoelectric sensor positioned diagonally across a traffic lane at a specified angle. Sensor output was a piezoelectric voltage signal characterized by a pulse for every passing tire. As aforementioned, in order to use collected data for vehicle classification, distinguishing features for various classifications must be extracted and input into a learning algorithm to generate another set of data, maximizing differentiation among classes to achieve accurate vehicle classification.

Raw signal—sampled at frequencies of 10Ksps or 1Ksps—is too large for classification processing and algorithm learning. Dimension reduction must first be performed. If accomplished through a rough under-sampling of the raw signal, a significant loss of information will occur. A more intelligent method should be employed to reduce data set size while maintaining the greatest amount of signal information possible.

One drawback of our single-element sensor design is its inability to estimate vehicle width track; hence, it is unable to determine vehicle speed or axle spacing. In this research, several methods for performing vehicle classification were developed to overcome this limitation. The first method is to assume an average vehicle width for all passing vehicles and calculate vehicle speed. Another novel method adapted for our system development was using the ratio of vehicle track width over its length (W/L). Figure 5.6 shows a voltage signal acquired from a class 5 vehicle. Time duration between first pulse and second pulse is proportional to vehicle width. Also, time duration between first pulse and third (penultimate) pulse is proportional to vehicle length. The ratio of w over l eliminates the effect of speed on the data, as shown in eq. (5.1). Given that we can constitute thresholds that separate data from distinctive classes, vehicle classification can be determined using this novel method.

$$\frac{w}{l} = \frac{T_{12}.V/\cot\theta}{T_{1p}.V} = \frac{T_{12}.\tan\theta}{T_{1p}} \quad (5.1)$$

Where:

w : track width

l : length

T_{12} : time duration between first pulse and second pulse

T_{1p} : time duration between first pulse and penultimate pulse

V : vehicle speed

θ : angle between piezoelectric sensor and traffic direction

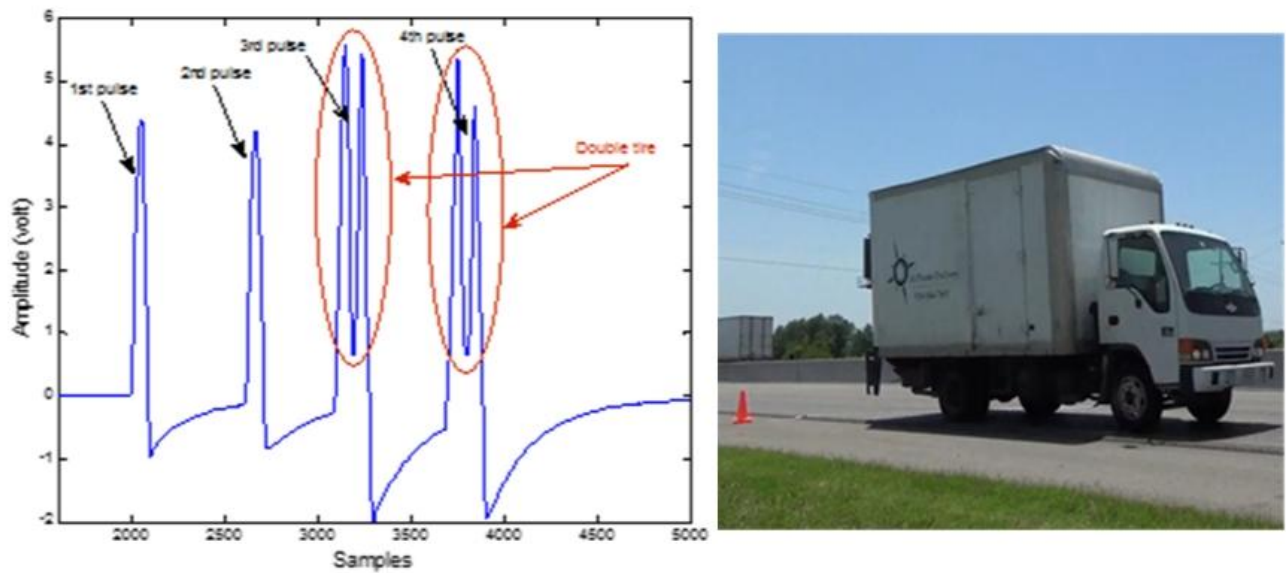


Figure 5.6. Class 5 data

Highway Deployments and Results

Single-element classification system testing and associated newly developed algorithms required performance assessment under realistic conditions. Four highway deployments (AVC10, AVC18, AVC47, and AVC19) were scheduled and performed on a variety of Oklahoma highways. Each deployment was performed within proximity of an Oklahoma Department Of Transportation (ODOT) automatic vehicle classifier (AVC) site. A Roadtrax BL piezoelectric sensor manufactured by Measurement Specialties was deployed diagonally across a traffic lane. For AVC47 deployment, a complete commercial-grade REECE-based system developed by the OU research team was deployed and evaluated. For AVC10 and AVC19 deployments, NI-9215 DAQ was used to collect data from the single-element sensor. Algorithms for determining axle spacing and vehicle lengths using (W/L) ratio was coded on MatLab. AVC18 deployment resulted in biased data due to deployment site features. A description and discussion of each deployment is detailed below.

Highway deployment at AVC47

AVC47 deployment utilized a Measurement Specialties Roadtrax Bl piezoelectric sensor affixed diagonally over the traffic lane at a 45° angle and a REECE device running the newly developed vehicle classification algorithm. The site of the deployment for the new system was adjacent to the ODOT AVC47 site, which contained the ADR unit. Vehicle classification data from ADR was recorded and collected in intervals of one minute for the duration of testing. Classification results of the single-element REECE were compared to ADR results. Total deployment time was 80 minutes.

Video footage was used as ground-truth data and compared with REECE device and ADR data. Table 5.2 lists classification results for all 13 FHWA classes and compares them with video ground-truth data. Notably, class 15 vehicles did not fall in a specific class. Class 14 data was reserved for future use.

The REECE device achieved an overall classification accuracy rate of 85.38% for vehicles, and 100% for class 1 motorcycles. Improved performance was indicated for vehicles in lower classes (e.g., passenger vehicles and lighter trucks). Heavier truck classification declined for class 9 and 6 vehicles. Analysis was not performed on erroneous data, e.g., when a class 9 vehicle combined with a class 2 vehicle and was

then erroneously classified as a class 13 vehicle; also, when a class 6 vehicle was misclassified as a result of error in tire detection. Instances such as these can be mitigated in future work by enhancing the classification algorithm to account for a non-formal number of pulses, as well as changing maximum axle spacing with respect to amount of traffic on highway and average speed.

Table 5.2. Classification results by REECE compared to ground truth and ADR at AVC47

Class	Video	ADR	Difference	REECE	Difference
	Lane 2	Lane 2	Lane 2	Lane 2	Lane 2
CI 1	2	2	0.00%	2	0.00%
CI 2	108	118	-9.26%	116	-7.41%
CI 3	88	64	27.27%	67	23.86%
CI 4	0	0	0.00%	0	0.00%
CI 5	3	17	-466.67%	0	100.00%
CI 6	6	6	0.00%	2	66.67%
CI 7	1	1	0.00%	3	-200.00%
CI 8	0	1	0.00%	3	0.00%
CI 9	4	4	0.00%	1	75.00%
CI 10	0	0	0.00%	0	0.00%
CI 11	0	0	0.00%	0	0.00%
CI 12	0	0	0.00%	1	0.00%
CI 13	0	0	0.00%	1	0.00%
CI 14	0	0	0.00%	0	0.00%
CI 15	1	0	100.00%	3	-200.00%

Highway deployment at AVC18

Data from AVC18 deployment was biased due to the non-uniform angle between approaching vehicles and the deployed piezoelectric sensor. Unknowingly, the system was inadvertently deployed directly after a highway entrance, which caused approaching vehicles to overpass the sensors from a variety of directions. Hence, the precise angle between sensor and traffic lane was unknown. Figure 5.7 depicts the deployment site. This deployment indicated that the angle of sensor placement is an extremely important parameter for data processing when using a diagonal sensor classification system. Usable classification results could not be extracted from data collected at AVC18. Again, this emphasizes the importance of proper deployment site.

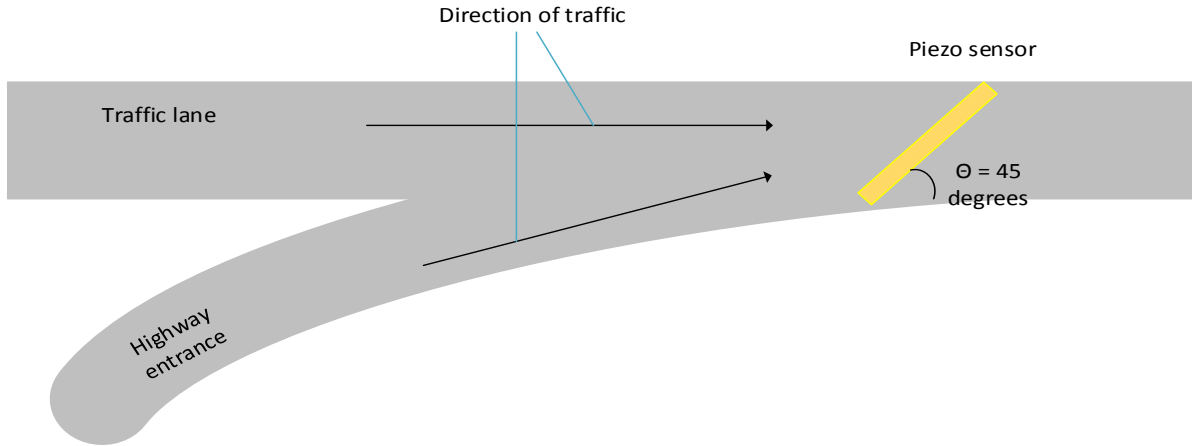


Figure 5.7. AVC18 deployment site schematic

Highway deployment at AVC10

AVC10 highway deployment utilized a piezoelectric sensor covering a traffic lane at a 45° angle on Oklahoma highway 169 in Tulsa, Oklahoma. Data from the sensor was collected using NI-9215 DAQ for 30 minutes. Data was processed using an assumed average width algorithm, as well as the W/L ratio presented earlier. Results were compared to ground-truth video data. Notably, data preprocessing was performed to remove incomplete data, e.g., when a vehicle changed lanes while driving over the sensor.

Table 5.3 details classification results for both average width and W/L ratio methods for each of the 13 FHWA vehicles, as well as classes 14 and 15 described earlier. The average width is assumed to be 5.78 ft for this analysis.

Table 5.3. Classification results for AVC 10

Class	Video	(W/L) Classification method	Error	Average width	Error
	Lane 1	Lane 1	Lane 1	Lane 1	Lane 1
CI 1	9	9	0.00%	12	-33.33%
CI 2	107	113	-5.61%	118	-10.28%
CI 3	94	96	-2.13%	76	19.15%
CI 4	0	0	0.00%	0	0.00%
CI 5	7	5	28.57%	2	71.43%
CI 6	49	43	12.24%	49	0.00%
CI 7	0	0	0.00%	0	0.00%
CI 8	2	2	0.00%	9	-350.00%
CI 9	39	39	0.00%	37	5.13%
CI 10	1	1	0.00%	3	-200.00%
CI 11	0	0	0.00%	3	0.00%
CI 12	0	0	0.00%	0	0.00%

CI 13	0	0	0.00%	0	0.00%
CI 14	0	0	0.00%	0	0.00%
CI 15	0	0	0.00%	9	0.00%

An 84.4% classification rate was achieved using the generic width algorithm. Several reasons for misclassification are existent. Some classes overlap in axle spacing, making it impossible to determine a threshold that completely distinguishes them. The accuracy of pulse detection can also affect vehicle classification.

Table 5.3 shows acceptable classification results with 0% error for classes 1, 8, 9, and 10 when using W/L ratio. Classification error for other classes is evident due to an overlap (same number of tires) between classes.

For each number of pulses, a W/L threshold was chosen to distinguish between classes. A threshold at the center of W/L values was first selected at mean value between W/L ratios of two classes to distinguish between those with the same number of pulses. Thresholds values were then adjusted to increase separation between classes. This improved distinction between classes. Thresholds employed are listed in Table 5.4.

Table 5.4. W/L thresholds used for vehicle classification for AVC10 deployment

Pulse number	Thresholds between classes					
	Classes 2,3	Classes 3,5	Classes 6,3	Classes 3,8	Classes 2,8	Classes 6,10
4	0.575	0.47	x	x	x	x
6	X	x	0.2724	0.19	x	x
8	0.1742	x	x	x	0.156	x
12	X	x	x	x	x	0.135

Highway deployment at AVC19

The AVC19 highway deployment was performed on Oklahoma highway I-44 using a piezoelectric sensor covering a traffic lane at a 40° angle. Duration of deployment was approximately 2 hours, 45 minutes and utilized NI-9215 DAQ. Like the AVC10 deployment, data was processed using both an average width algorithm and W/L ratio. Results were compared to ground-truth video data. Classification results for both average width and W/L ratio are presented in Table 5.5. W/L thresholds used for vehicle classification for AVC19 are presented in Table 5.6.

Table 5.5. Classification results for AVC 10

Class	(W/L) Classification method		Error	Average width	Error
	Video Lane 1	Lane 1	Lane 1	Lane 1	Lane 1
CI 1	5	5	0.00%	31	-520.00%
CI 2	536	538	-0.37%	582	-8.58%

CI 3	322	321	0.31%	260	19.25%
CI 4	2	2	0.00%	0	100.00%
CI 5	46	42	8.70%	0	100.00%
CI 6	36	38	-5.56%	38	-5.56%
CI 7	2	2	0.00%	2	0.00%
CI 8	9	10	-11.11%	13	-44.44%
CI 9	118	118	0.00%	101	14.41%
CI 10	1	1	0.00%	2	-100.00%
CI 11	1	2	-100.00%	0	100.00%
CI 12	1	1	0.00%	0	100.00%
CI 13	2	1	50.00%	0	100.00%
CI 14	0	0	0.00%	0	0.00%
CI 15	0	0	0.00%	63	0.00%

Table 5.6. (W/L) thresholds used for vehicle classification for AVC10 deployment

Thresholds between classes												
Pulse number	Classes 2,3	Classes 3,5	Classes 4,5	Classes 4,6	Classes 6,3	Classes 6,8	Classes 3,8	Classes 7,8	Classes 8,9	Classes 9,11	Classes 10,12	Classes 6,13
4	0.6342	0.53	0.385	0.333	x	x	x	x	x	x	x	x
5	0.275	x	x	x	0.39	x	x	x	x	x	x	x
6	x	x	x	x	x	0.31	0.305	x	x	x	x	x
8	x	x	x	x	x	x	x	0.18	0.14	x	x	x
9	x	x	x	x	x	x	x	x	x	0.13	x	x
11	x	x	x	x	x	x	x	x	x	x	0.1202	x
12	x	x	x	x	x	x	x	x	x	x	x	0.135

An 80.6% classification accuracy rate was achieved using the average width algorithm. Performance declined when compared to AVC10 deployment. The change in sensor position angle affected pulse detection, e.g., detection of three pulses for class 2 and 3 vehicles instead of four pulses corresponding to four tires. Pulses from the second and third tires were combined into one pulse. Thus, the pulse detection algorithm was modified for improvement by using two different pulse windows—a smaller one for classes 2 and 3 and larger one for higher numbered classes. Changing the pulse detection algorithm reduced errors significantly. However, pulse detection remained prone to error for some vehicles. For example, 26 vehicles classified as motorcycles had three detected pulses. In our algorithm, three-pulse vehicles are classified as motorcycles to accommodate three-tire motorcycles. We concluded that if an angle of less than 45° is used, the average width algorithm used to classify a vehicle with three detected pulses should be changed to indicate class 2 vehicle classification.

Class 1, 4, 7, 9, 10, and 12 had a 100% accurate classification rate. Classification errors for other classes were clearly due to an overlap between them.

Principal component analysis

Principal Component Analysis (PCA) has traditionally been used for feature extraction and data dimension reduction technique. PCA uses mathematical techniques to transform correlated data in domain of orthogonal components. Few primary principal components contain information required to distinguish data observations from one another [13].

Covariance matrix V of the available vehicle data must be constructed to obtain Principal Components (PCs) of the data [14]. Matrix diagonal represents the variance of data observed for each vehicle, while other elements represent the covariance between observations corresponding to different vehicles. To find V , a modified data matrix X , in which the ensemble mean x is removed, must be found. Let x^p be a vector of length N that contains data for the p th vehicle, where $p = 1, \dots, M$, and M is the total number of vehicles. Data matrix X (M by N) can then be constructed, where each column of matrix X is a vehicle data vector x^p . To construct X , one must calculate x and then subtract the result from all vehicle vectors x^p . See equations (5.2, 5.3, and 5.4)

$$x = \frac{\sum_{p=1}^M x^p}{M} \quad (5.2)$$

$$x^p = x^p - x \quad (5.3)$$

$$X = (x^1, x^2, \dots, x^M) \quad (5.4)$$

As a result, we can calculate V , which will be of size ($N \times N$), by using X by its transpose X' :

$$V = X'X \quad (5.5)$$

Eigenvectors of V , (g_1, g_2, \dots, g_N), are then computed and associated with eigenvalues ($\lambda_1, \lambda_2, \dots, \lambda_N$). The latter are placed in descending order where the highest eigenvalue represent the highest variance between data observations. The eigenvectors associated with eigenvalues represent the principal components of the data.

After finding PCs, a calculation will be determined to select learning methods for vehicle classification. A number of PCs will be used to extract k features from total N samples for each vehicle data. The first k PCs with sufficient information about the original signal will be chosen. This figure can be found by examining the first k eigenvalues as they carry the information explaining the variance of data observation for the first k PCs. Features can be calculated using the following equation:

$$f^p = x^p [g_1, g_2, \dots, g_k] \quad (5.6)$$

Our data consists of $M = 308$ vehicles signals of different classes where each signal is 12,001-long samples obtained at 10KS/s. Table 5.7 details number of vehicles in each class. Signal was down converted to 1KS/s to facilitate simpler data handling without significant loss of information and to yield a signal length of $N= 1,201$ for each vehicle. The sensor was positioned at a 45° angle to traffic direction.

Table 5.7. Number of each class in data set

Class	1	2	3	5	6	8	9	10
Number of vehicles	9	107	94	7	49	2	40	1

PCA procedure was performed on the available data set. As mentioned earlier, a small set of the total number of PCs, when compared to total signal size, is ample for generating a feature that encompasses a large percentage of those used to distinguish vehicles from one another. Figure 5.8 shows data variance for the first 308 PCs, i.e., percentage of features contributed by each PC. Notably, the total number of PCs equals $N = 1,201$; however, PCs greater than the number of vehicles, i.e., $M = 308$, are insignificant. The first 308 PCs explains 100% of the variance. Hence, they retain 100% of features required for extraction. Variance percentage declines exponentially as the number of PCs increases.

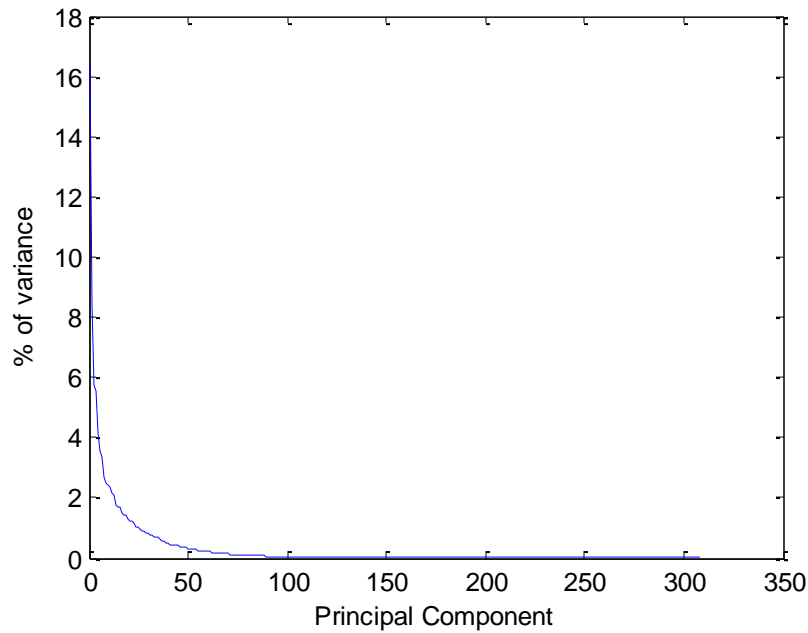


Figure 5.8. Percentage of variance of data for PCs

Utilizing 50 PCs covers 92.6816% of the signal. Figure 5.9 shows a comparison between an original class 2 signal and a reconstructed one when using 50 PCs to compress vehicle signal.

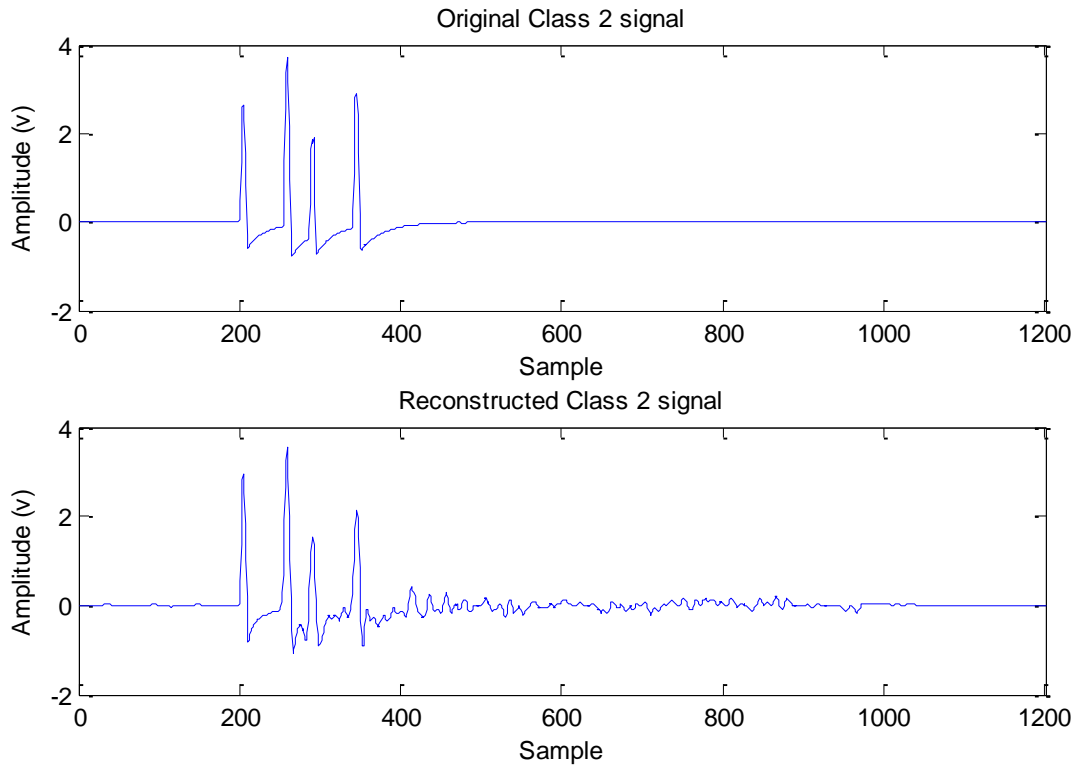


Figure 5.9. Class 2 original signal and reconstructed signal

Vehicle classification using PCA and Bays networks including W/L ratio

A relatively large sample of vehicle data representing different classes must be collected to determine if and how effectively thresholds are able to distinguish vehicle data.

A piezoelectric sensor covering a traffic lane at a 45° angle was deployed on Oklahoma highway 169. Sensor data was acquired for approximately 30 minutes.

To associate each signal with its corresponding class, it was imperative to use a ground-truth data system. For this purpose, a video camera was installed to record highway traffic during deployment. Video recording was processed to classify passing vehicles and associate them with corresponding voltage signals. Notably, data preprocessing was performed to remove incomplete data, e.g., when a vehicle changed lane.

Figure 5.10 shows that data is more distinguishable when pulse number is corresponded with tire number and plotted against W/L ratio. An overlap is apparent for lighter vehicles, such as classes 2, 3, and 5. However, heavier trucks, such as classes 6 and 9, are better distinguished from other traffic data. Also, many class 2 and 3 vehicles generate more than four pulses when attached to some type of trailer. Classification in this situation will be challenging.

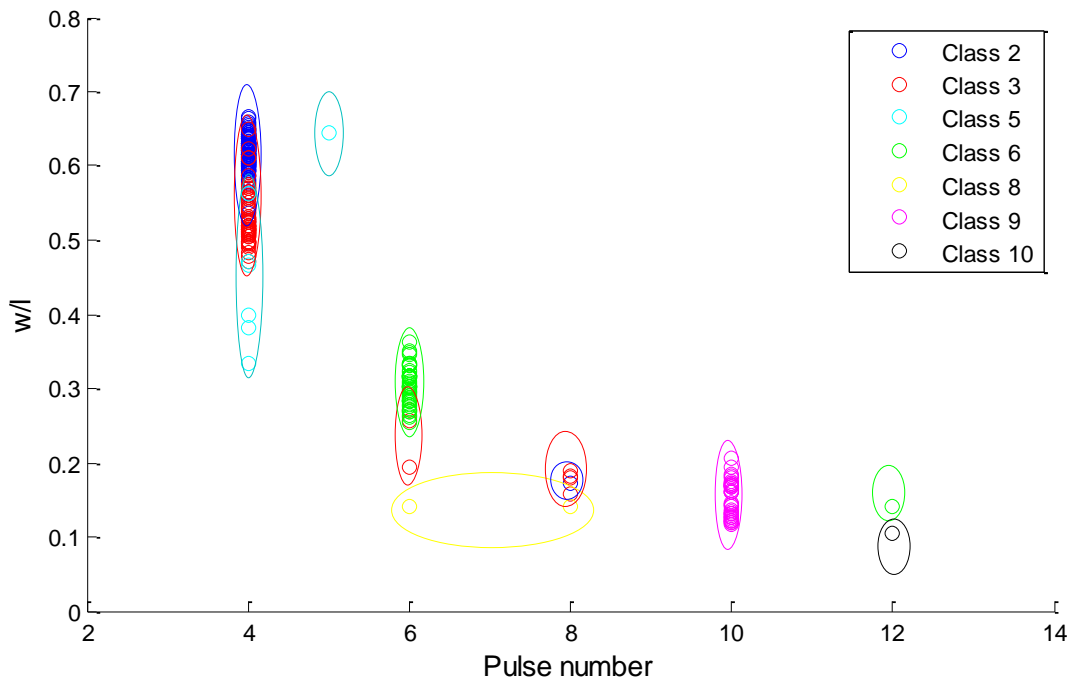


Figure 5.10. Pulse number vs. W/L ratio

Utilization of W/L ratio and pulse number will be examined with 50 feature extracted using PCA.

These features will establish the input vector for the Bayesian learning method used to perform vehicle classification. Bayesian Networks or Belief Networks (BN) are a hybrid of graph theory and probability theory. BN is a directed acyclic probabilistic graphical models consisting of a node at which a conditional probability distribution is defined, as is the probabilities of directed paths between nodes. Learning with BN aims to determine structures and conditional probabilistic tables between nodes by using input training data [15-16].

A preliminary test was performed using our data and BN. A random learning sample of 154 was chosen to train the network. Results were subsequently tested on our data set. Experiments had a number of features, including:

- Test 1 included 52 features that corresponded to 50 features extracted by PCA, W/L ratio, and pulse number
- Test 2 included 51 features—50 features extracted by PCA and W/L ratio
- Test 3 included only 50 features extracted by PCA
- Test 4 included 51 features—50 features extracted by PCA and pulse/tire number

Classification results for selected features are presented in Table 5.8.

Table 5.8. Classification results using PCA and bays network on single element piezo-sensor

	Test 1	Test 2	Test 3	Test 4
	Classification Accuracy Percentage			
Total Classes	90.29	90.94	88.03	89
Class 1	100	100	100	100
Class 2	89.57	90.35	81.75	81.89
Class 3	93.98	94.12	93.59	94.81
Class 5	37.50	40	85.71	85.71
Class 6	100	100	90.57	94.12
Class 8	100	100	100	100
Class 9	93.02	93.02	92.68	93.02
Class 10	0	0	0	0

A superior classification rate of 90.94% was achieved with test 2 when using 50 PCA extracted features and W/L ratio. Classification for class 2 vehicles was unsurpassed, most likely because this class had the largest number of vehicles in the data set. Class 5 vehicles had the poorest classification results in test 2. However, class 5 classification was improved in test 4 when using 50 features extracted by PCA and pulse number, although class 2 had a lower classification rate. This phenomenon can be explained by the significant overlap in class 5 in test 2. Class 2 and 3 vehicles had overlap in test 4 with regard to W/L ratio, e.g., approximately 42% of class 5 vehicle were overlapped.

A classification rate of 100% was achieved for classes 1, 6, and 8 in all tests. In future experiments, classes with a lower rate of success, e.g., class 8 and 10, could possibly be omitted, because they could bias feature extraction using PCA. It is important to remember that a classification rate of 100% for class 1 motorcycles is obtained simply by observing the two pulses. Motorcycles are the only class with two pulses. Hence, we suggest it is prudent to classify motorcycles independently from other vehicles.

Errors reported when processing Single-element data

This section explains the three types of errors encountered during classification processing of data obtained from the single-element sensor.

Type 1 Error: No Pulses in Signal Data

In Type 1 Error, a vehicle is captured on video crossing the sensor; however, no pulses were recorded in the signal data. For AVC19 deployment, 11 out of 1,128 vehicles were characterized without a pulse, resulting in 0.975% of Type 1 Error. Figure 5.11 clearly shows a class 2 vehicle crossing over the sensor. Review of the video confirms that the vehicle crossed over the sensor without switching lanes.



Figure 5.11. Picture of class 2 vehicle missed by the sensor of Frame 16641

Table 5.9 is a record of the video data. Indicators validate that a class 2 vehicle was recorded crossing the sensor in frame 16641.

Table 5.9. Example of missed vehicle within vehicles from Frames 15376 through 17012

Video File Name	Lane	Class	Frame	Is Recreational	Time	Actual Time
MAH00037.MP4	1	2	15376	0	00:08:33	12:07:30
MAH00037.MP4	1	2	15546	0	00:08:38	12:07:35
MAH00037.MP4	1	9	15792	0	00:08:46	12:07:43
MAH00037.MP4	1	3	16167	0	00:08:59	12:07:56
MAH00037.MP4	1	2	16217	0	00:09:01	12:07:58
MAH00037.MP4	1	3	16303	0	00:09:04	12:08:01
MAH00037.MP4	1	2	16641	0	00:09:15	12:08:12
MAH00037.MP4	1	9	16980	0	00:09:26	12:08:23
MAH00037.MP4	1	3	17012	0	00:09:27	12:08:24

Figure 5.12 shows signal data from vehicles in Table 1.1. The numbers above each signature denote to which class of vehicle the signature belongs. Matching the record data from Table 1.1 to the signal data reveals no pulses for the class 2 vehicle appearing in the frame. The location at which pulses should be present is denoted in red. The cause for missing pulses is unclear.

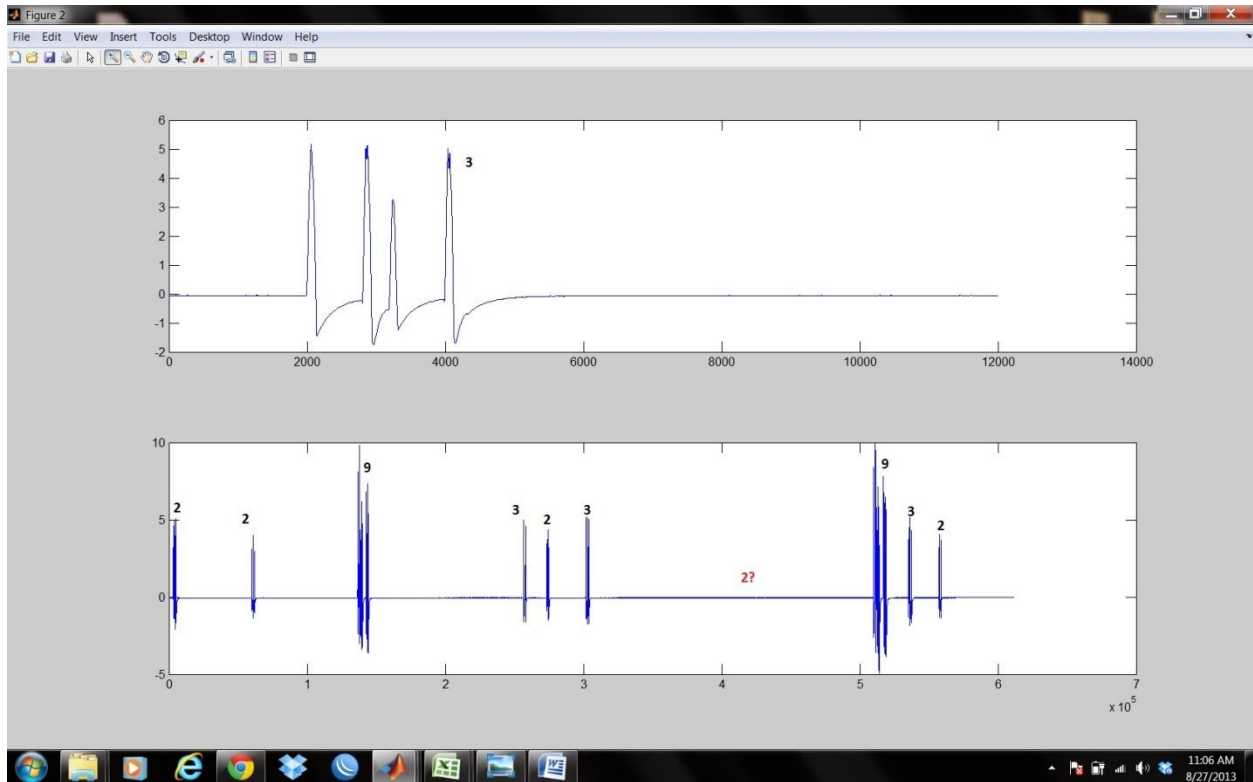


Figure 5.12. Example of a vehicle signal missed by sensor

Type 2 Error: Extra Pulses in Signal Data

In Type 2 Error, pulses are evident in the signal data but no vehicle is shown crossing the sensor in the video data. For AVC19, an excess of 14 signals were indicated for 1,128 vehicles. This phenomenon resulted in a 1.241% error.

Figure 5.13 validates that a class 2 vehicle is not apparent before the vehicle shown in the frame. Data recorded in the next table reveals that no class 2 vehicle was recorded as crossing the sensor before the vehicle in frame 42593. However, the subsequent figure of pulses reveals an excess of pulses before the class 2 vehicle in frame 42593. Video footage reveals that the white class 2 vehicle in Figure 5.14 crossed the sensor before the black class 2 vehicle in frame 42593. The program for recording the video data failed to detect and record the white class 2 vehicle.



Figure 5.13. Frame 42593



Figure 5.14. Saved Image before Frame 42593

As stated previously, Table 5.10 contains no record of a class 2 vehicle crossing the sensor directly before the class 2 vehicle captured in frame 42593. The following figure conflicts with this data.

Table 5.10. Vehicles from Frames 42418 through 43486

Video File Name	Lane	Class	Frame	Is Recreational	Time	Actual Time
MAH00037.MP4	1	9	42418	0	00:23:35	12:22:32
MAH00037.MP4	1	6	42461	0	00:23:36	12:22:33
MAH00037.MP4	1	2	42593	0	00:23:41	12:22:38
MAH00037.MP4	1	2	42799	0	00:23:48	12:22:45
MAH00037.MP4	1	2	43096	0	00:23:57	12:22:54
MAH00037.MP4	1	5	43486	0	00:24:11	12:23:08

Figure 5.15 displays the signal data from vehicles in Table 5.10. The numbers above each signature denote the class to which each vehicle signature belongs. Matching the record data from Table 5.10 to the signal data reveals an extra set of pulses (denoted by a red number) before the class 2 vehicle captured in frame 42593. This extra set of pulses in Figure 5.14 demonstrates that the white class 2 vehicle was not successfully detected and recorded by the video data program.

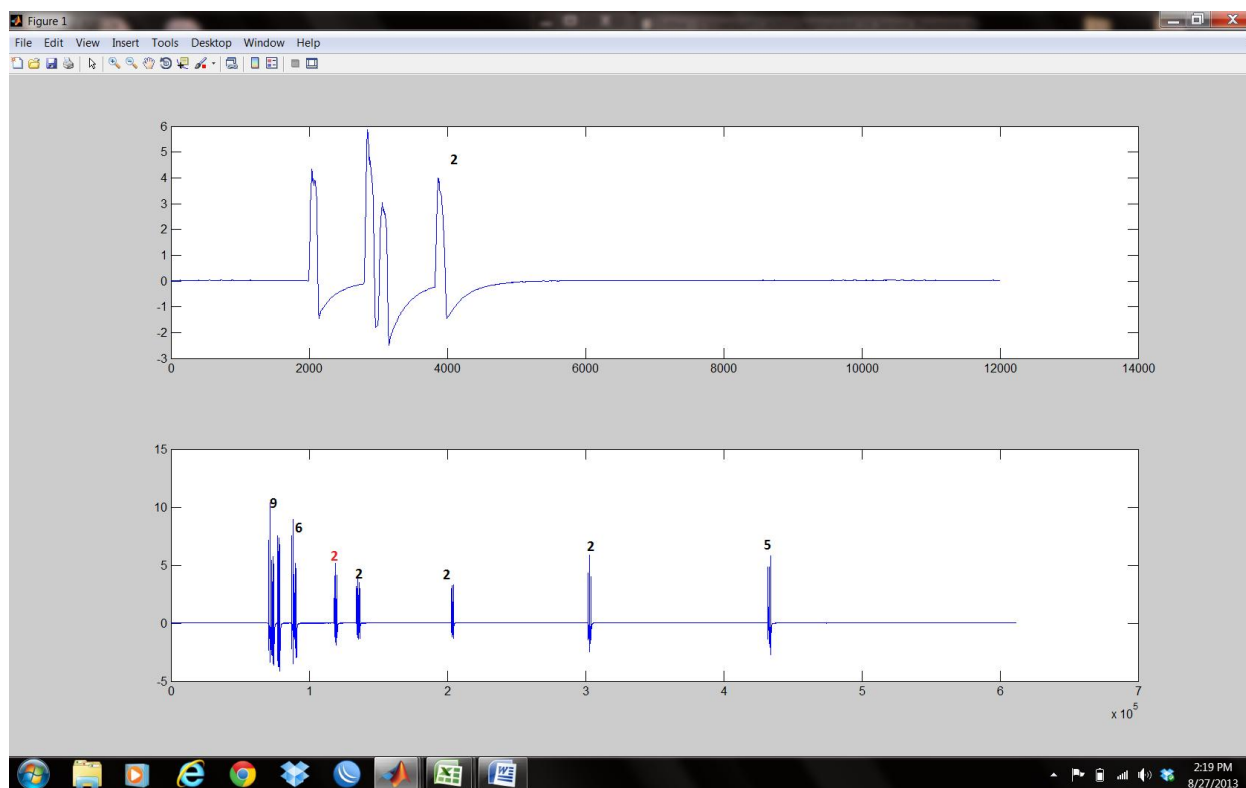


Figure 5.15. Pulses from Frames 42418 through 43486

Type 3 Error: Distorted Pulses

In Type 3 Error, signal data pulses match video data in which a vehicle crosses the sensor; however, pulses are fewer than expected. Typically this phenomenon is the result of a vehicle changing into another lane as it crosses the sensor. This section also illustrates another example of Type 2 Error discussed in the previous section. Files containing distorted pulses were not marked as distorted, so no percent error is calculated for Type 3 Error.

Figure 5.16 displays a class 6 vehicle at frame 13303. Although the following table shows that a class 9 vehicle crossed the sensor before the class 6 vehicle, video footage reveals that a class 3 vehicle changed to lane 2 while crossing the sensor ahead of the class 6 vehicle. Figures 5.17 and 5.18 display the vehicle as it changes lanes.



Figure 5.16. Frame 13303



Figure 5.17. Saved Image before Frame 13303



Figure 5.18. Saved Image before Frame 13303

Table 5.11. Vehicles from Frames 12857 through 14071

Video File Name	Lane	Class	Frame	Is Recreational	Time	Actual Time
MAH00037.MP4	1	9	12857	0	00:07:09	12:06:06
MAH00037.MP4	1	6	13303	0	00:07:23	12:06:20
MAH00037.MP4	1	2	13327	0	00:07:24	12:06:21
MAH00037.MP4	1	6	13584	0	00:07:33	12:06:30
MAH00037.MP4	1	2	13651	0	00:07:35	12:06:32
MAH00037.MP4	1	2	14071	0	00:07:49	12:06:46

As stated previously, Table 5.11 contains no record of a class 3 vehicle crossing the sensor directly before the class 6 vehicle in frame 13303. The following figure conflicts with this data.

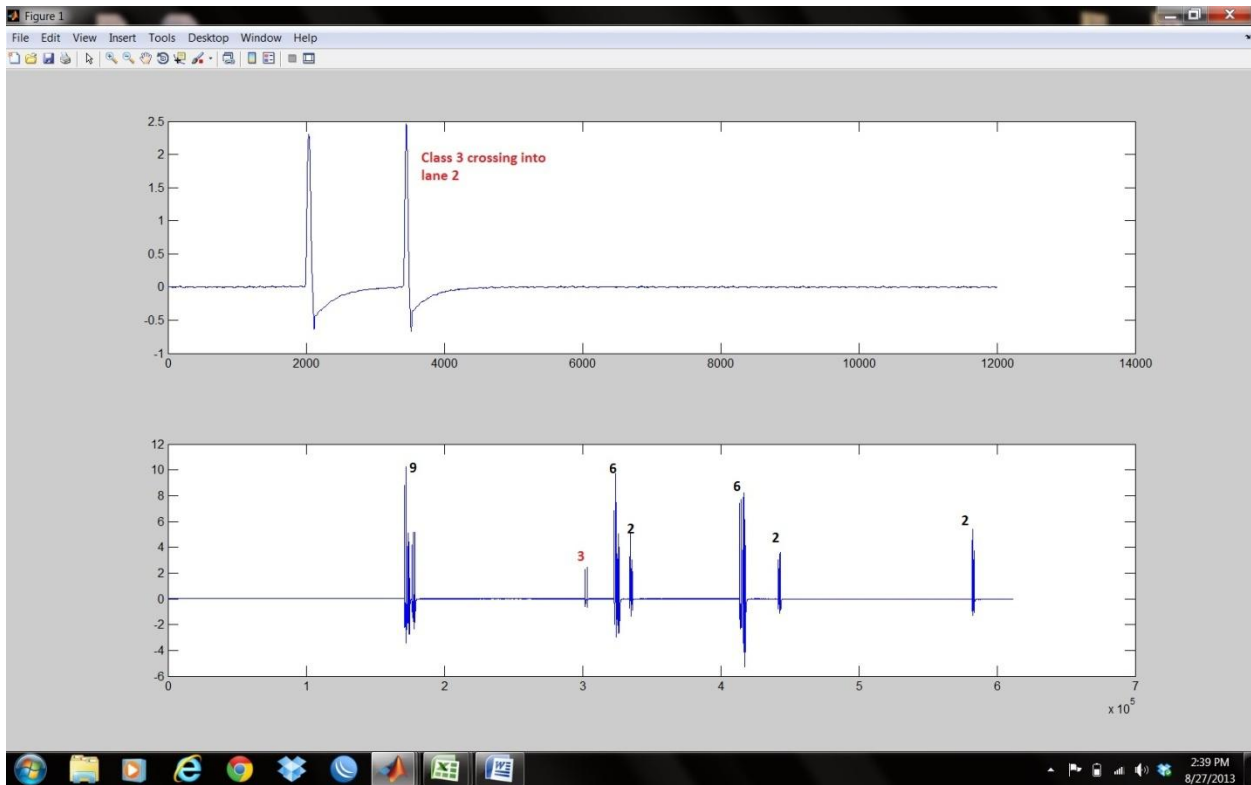


Figure 5.19 Pulses from Frames 12857 through 14071

Figure 5.19 displays signal data from vehicles listed in Table 5.11. The numbers above each signature denote to which class of vehicles the signature belongs. Matching the record data from Table 5.11 to the signal data reveals that there is an extra set of pulses (denoted by a red number) before the class 6 vehicle in frame 13303. The extra set of pulses is the result of the class 3 vehicle pictured in Figures 5.17 and 5.18 as it switched lanes when crossing the sensor. Lane changes caused two pulses instead of four (Type 3 Error) since only two tires hit the sensor. This also caused Type 2 Error because the sensor picked up two pulses from the class 3 vehicle while the video data program failed to detect and record the vehicle changing lanes.

Chapter VI

Multi element system development and highway testing

This chapter reviews software design and classification results obtained during highway testing of the multi-element vehicle classification system developed by PI Dr. Refai and his research team. The system was developed to accurately classify motorcycles and other vehicles according to FHWA class specifications. System performance under highway conditions was necessary, and collected data had to be processed accordingly. Highway deployment requires suitable sensor packaging, as it houses 16 sensor elements and their cabling, each measuring 1.5 ft long.

Data collected from sensors triggered by passing vehicles should be processed to extract vehicle parameters such as width, velocity, axle spacing, and length. These features can then be used to classify each vehicle. Algorithms used for processing data, extracting features, and making a classification decision will be presented in the following section.

Algorithms

This section describes the algorithm employed to process a multi-element sensor signal. The algorithm is divided into three major modules: pulse extraction, feature extraction, and classification. A description of each module and accompanying flow graph is provided in the following subsections. The algorithm was coded using Matlab.

Pulse extraction

The pulse extraction module detects pulses corresponding to tires impacting the sensor. This module reads raw data samples and determines peak amplitude for each channel, which aids decision-making about the impacted channel. Data compare sample amplitude sequentially to a threshold for all channels to detect pulses corresponding to vehicle tires. The algorithm then generates an index log of pulse start and stop times to calculate pulse duration, as well as peak amplitude value. Figure 6.1 offers a flow chart of the algorithm developed to identify all pulses captured on all channels. Algorithm detects peaks in the acquired signal and compares peaks from different channels with each other to make a decision on which channels were impacted. Then algorithm starts peak detection where it scans for amplitude higher than or equal to 25% of the peak detected amplitude value. Algorithm then finds the indices of start and end and peak value of each pulse and saves them.

Pulse Extraction Module

Max: The highest value that we have for our signal.

By using this procedure We can have a table with 3 values for each peak which are more than $0.25 * \text{Max}$:

- 1- Index of point which passes $0.25 * \text{Max}$
- 2- Amplitude of Peak
- 3- The index of Peak

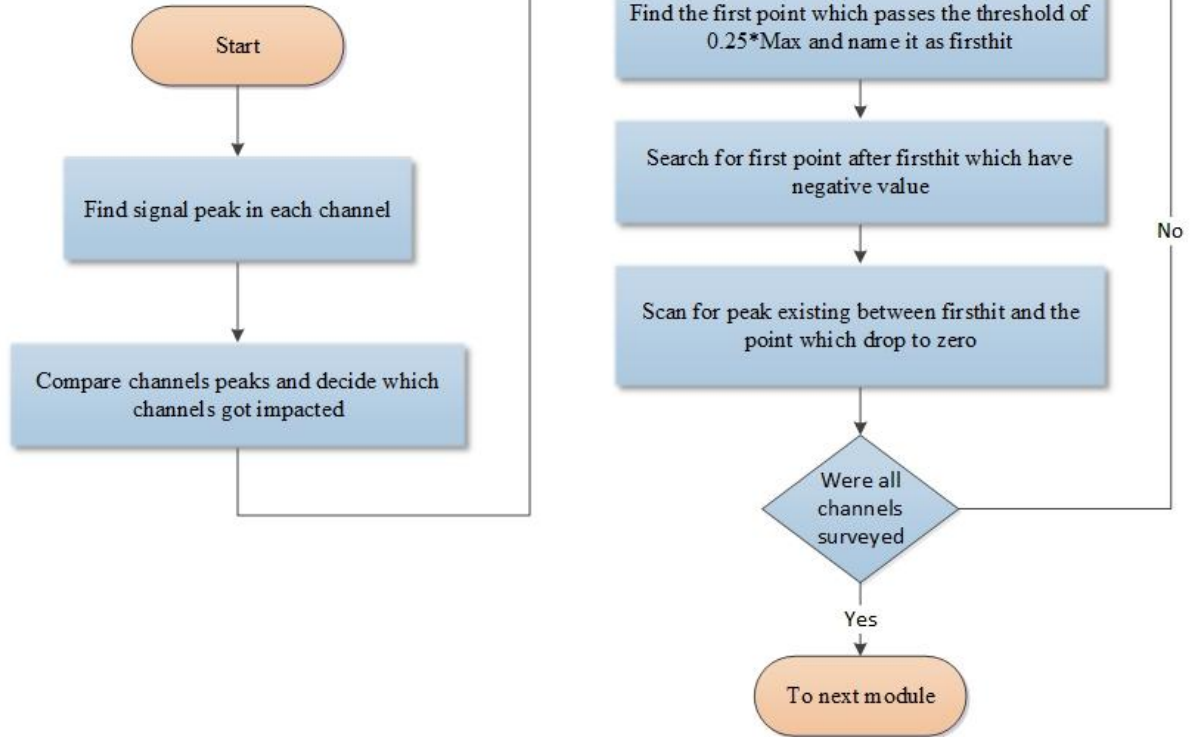


Figure 6.1. Pulse extraction module

Feature extraction

The feature extraction module is extremely important, as it calculates features required by the subsequent vehicle classification module. This module reads output delivered by the pulse extraction module and calculates vehicle width based on impacted elements. If multiple adjacent sensor elements were impacted, the distance between tires is calculated based on the midpoint of the group of sensors impacted. Depending on tire size and angle of deployment, multiple adjacent sensors could be impacted by crossing vehicles. The potential for impacting more sensor elements increases as the angle of deployment decreases from 90° (perpendicular to traffic) toward 0° (in line with traffic, i.e., not an valid angle).

Once the separating distance between two sensors impacted by tires belonging to the same axle is determined, the algorithm calculates speed using time difference between detected pulses corresponding to the tires. Eventually, having acquired speed, the algorithm can then calculate vehicle length and axle spacing between consecutive axles. Pulse indexes from one impacted element can be used to perform this task, as they correspond to consecutive axles of the same vehicle. Consult Figure 6.2 for a flow chart of the feature extraction module. Feature extraction module commences by finding the first impacted channel, and then dividing impacted channels into two groups. If only one channel was impacted then the

vehicle is classified as a motorcycle. If more than one, then algorithm calculates vehicle track width using sensor angle and tires indices from the two channel groups corresponding to the two front tires. Based on track width, speed can then be calculated. Finally, speed and pulses indices indicate vehicle length and axle spacing. Algorithm calculates and passes to classification module for classification decision.

Feature Extraction module

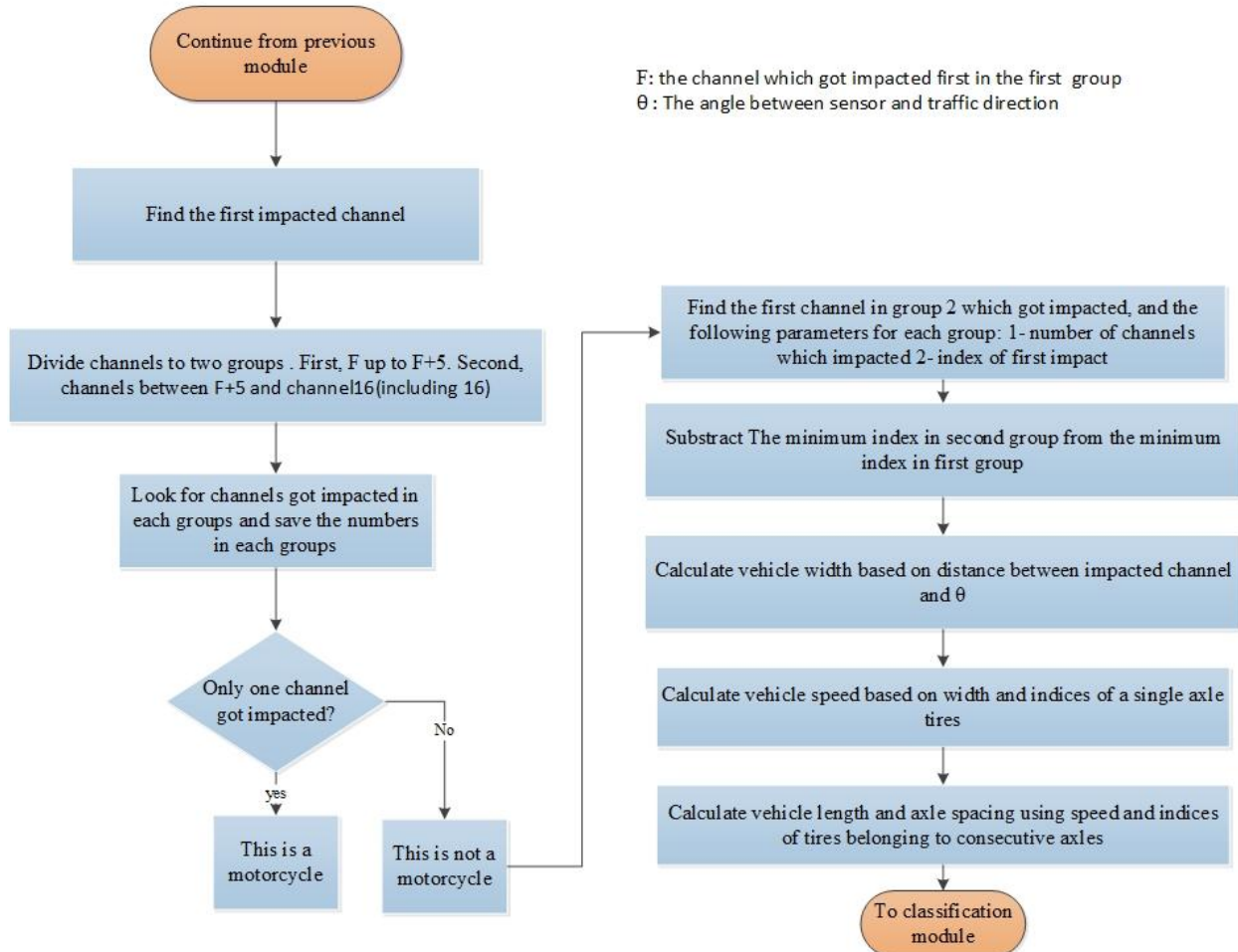


Figure 6.2. Feature extraction module

Vehicle classification

The primary goal of the work detailed in this report is building a system to classify vehicles, primarily motorcycles. The vehicle classification module receives data from the feature extraction module to execute vehicle classification. The algorithm employed for this module is based upon vehicle length, axle spacing, and number of tires. Axle spacing thresholds from Diamond Traffic were initially employed to differentiate between classes. The thresholds were later modified according to test results to improve differentiation. Table 6.1 shows thresholds ultimately developed and employed.

Table 6.1. Thresholds used in multi-element classification algorithm

Bin	Axles	Axle spacing (consecutive axles spacing separated by comma)
2	2-3	0-6.8, 10-18.8
3	2-3	6.8-9.5, 10-18.8
5	2	9.5-12.5
4	2-3	12.5-24, *
8	3	*, 18.1-99.9
6	3	*, 1-15
2	4-5	0-6.8, *, 1-1.9, 1-3.4
3	4-5	6.8-10, *, 1-3.4, 1-3.4
8	4	*, 5.1-99.9, 3.5-99.9
8	4	*, 1-5, 10-99.9
7	4	*, *, *
9	5	*, *, *, *
10	6	*, 3.5-8, 3.5-8, *, 8.1-99.9
12	6	*, *, *, *, 8.1-99.9
10	6-10	*, *, *, *, 3.5-8, 3.5-8, 3.5-8, 3.5-8, 3.5-8
13	6-10	otherwise

Highway deployments and results

This section describes highway deployment carried out to assess the vehicle classification algorithm and its results for the newly developed multi-element vehicle classification system. AVC19 site on Oklahoma highway I-44 was selected for deployment. Testing included six separate intervals totaling 2 hours, 45 minutes. The signal for the first five intervals was acquired at a sampling rate of 5kS/s. Sampling rate for the final interval was increased to 10kS/s.

Extensive work was required to construct sensor packaging, which included a 16 piezoelectric sensor element housed in road pocket tape connected to the DAQ module via 100ft coaxial cable for each sensor element. Cables were channeled to roadside inside road pocket tape, and then connected to the NI-9205 DAQ unit. The principal pocket road tape housed sensor elements deployed at a 30° angle to traffic direction. Secondary pocket road tapes were employed to channel connecting cables. Figure 6.3 demonstrates the deployment site and sensor layout.



Figure 6.3. AVC19 deployment site and sensor layout

Data was preprocessed to eliminate irregularities, such as an incomplete signal resulting from a vehicle changing lanes.

Sixteen sensor elements are required to cover a 12ft traffic lane at a 30° angle diagonal layout. Unfortunately, sensor element 3 was damaged during transportation to the testing site, and its data was removed from results. This occurrence allowed the research team to assess fault tolerance of the system and its ability to utilize fewer elements while maintaining a high level of accuracy. Figure 6.4 depicts an example of aligned signal for passing vehicles collected from 15 sensor elements.

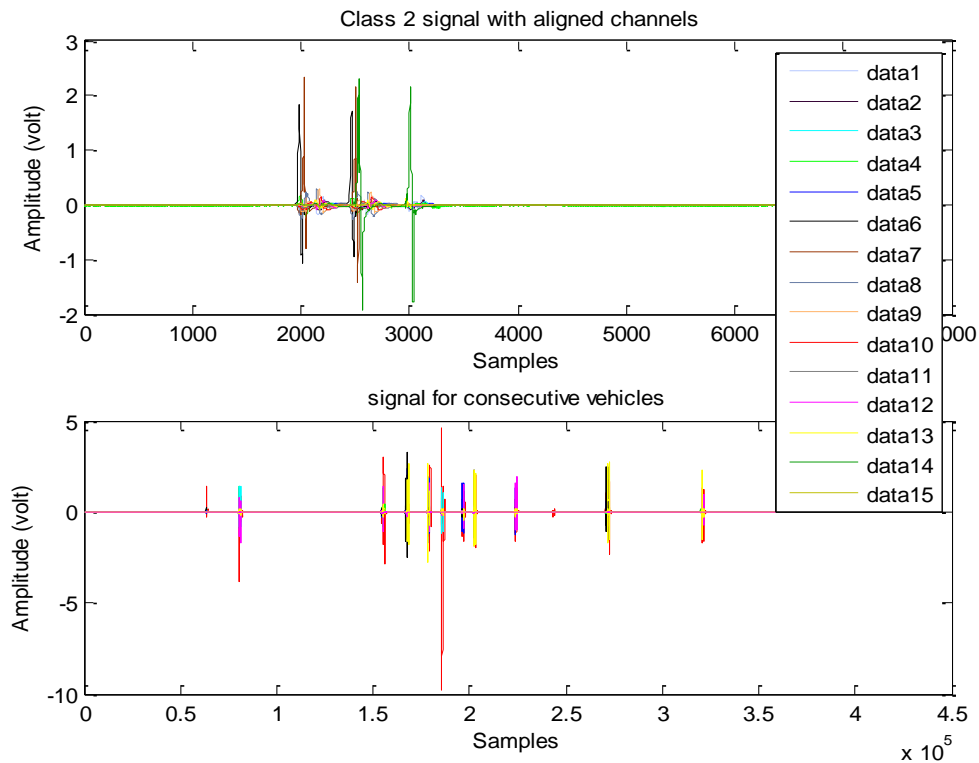
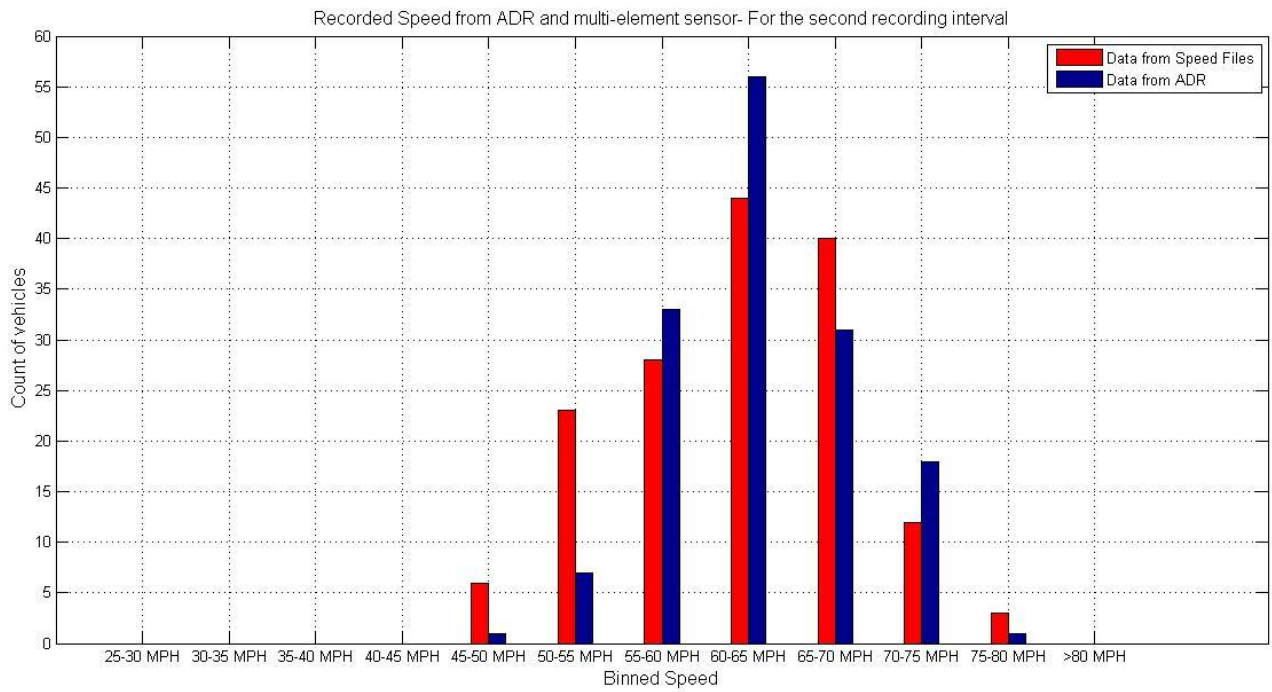
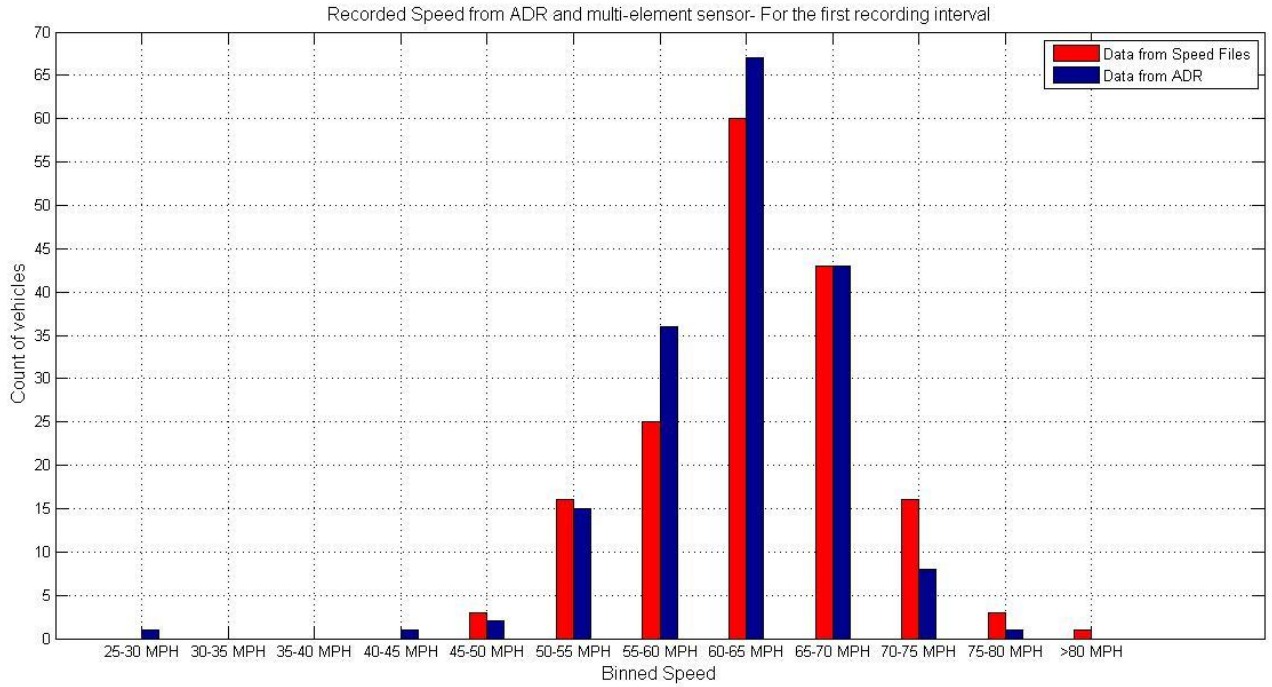
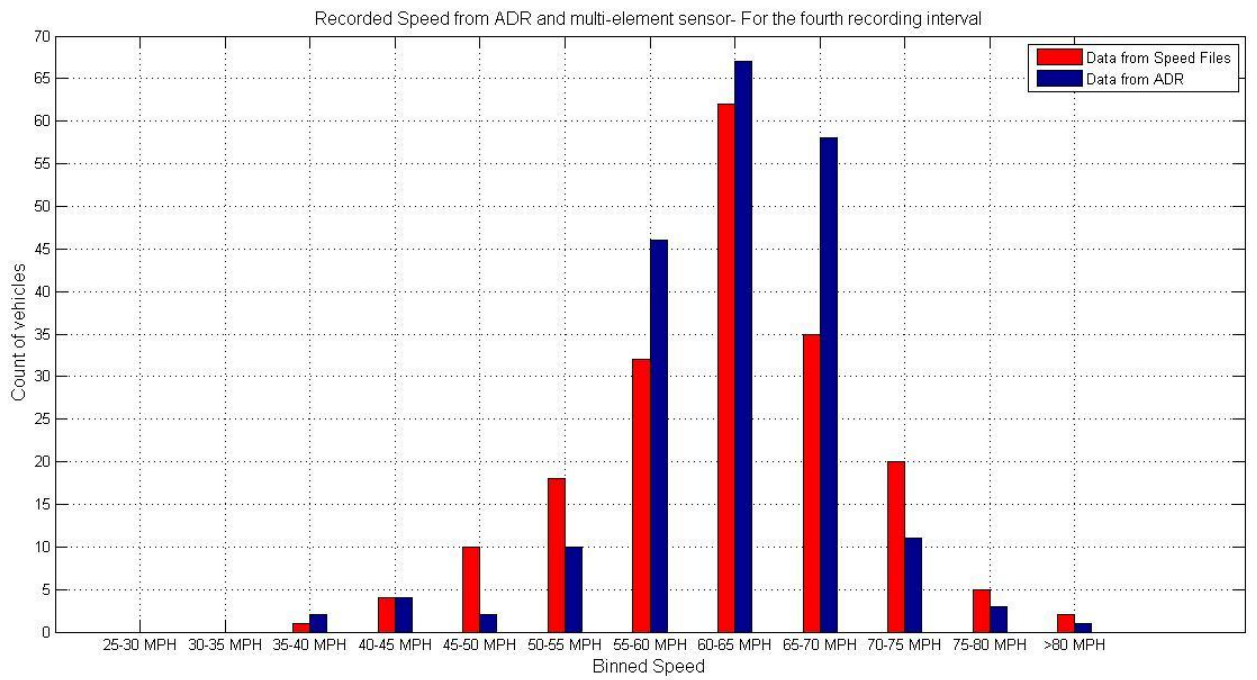
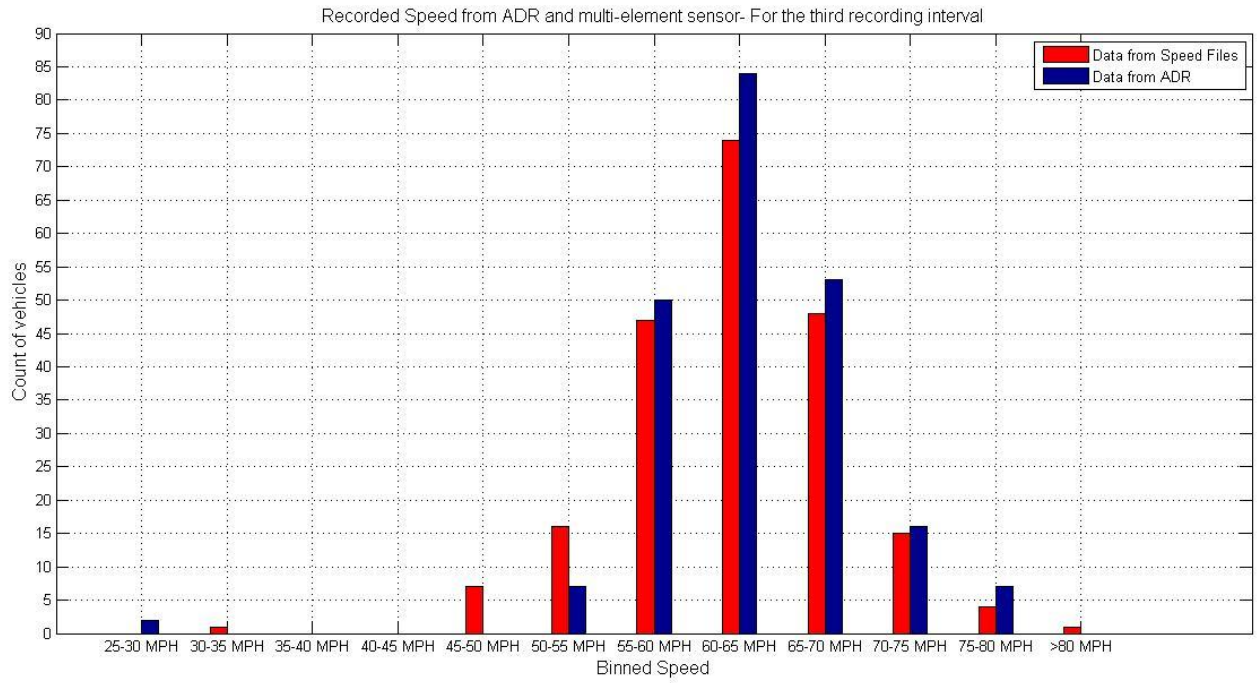


Figure 6.4. Raw signal from 15 aligned elements for class 2 vehicle

The algorithm was applied on data for all passing vehicles to calculate speed during corresponding test time intervals. A distribution of calculated speed was then plotted and compared with ADR speed for the six test intervals. Figure 6.5 compares the speed distribution calculated by the multi-element sensor and the ODOT ADR system.





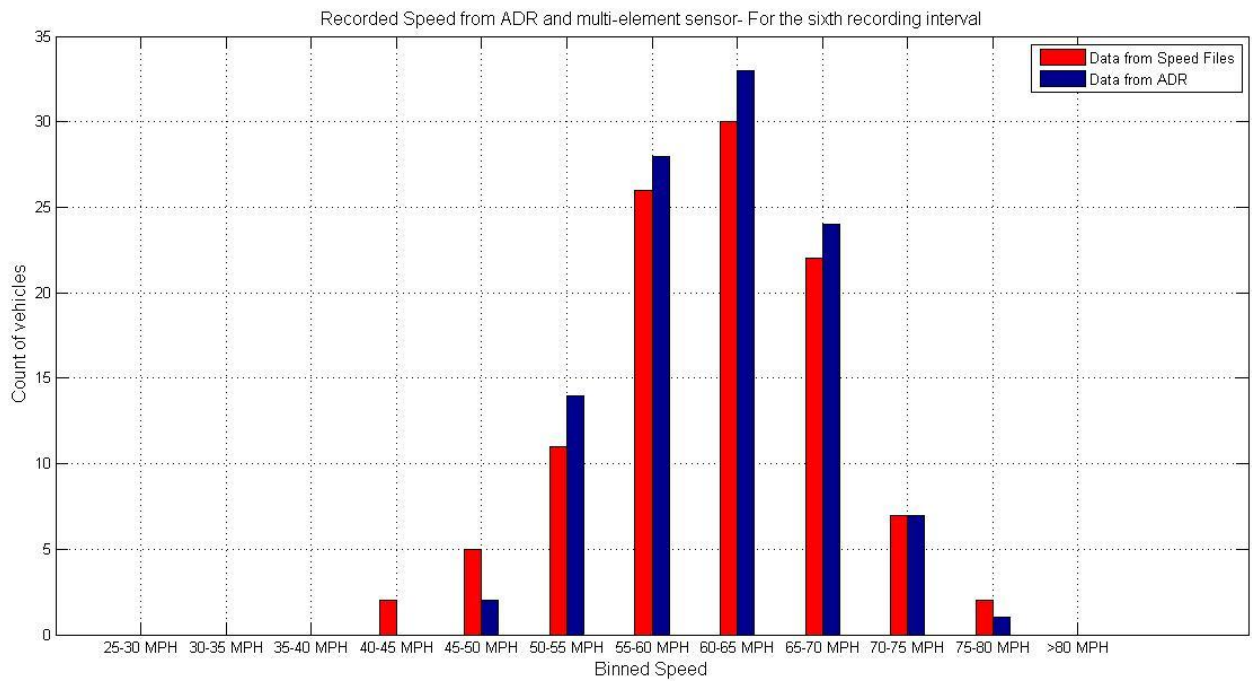
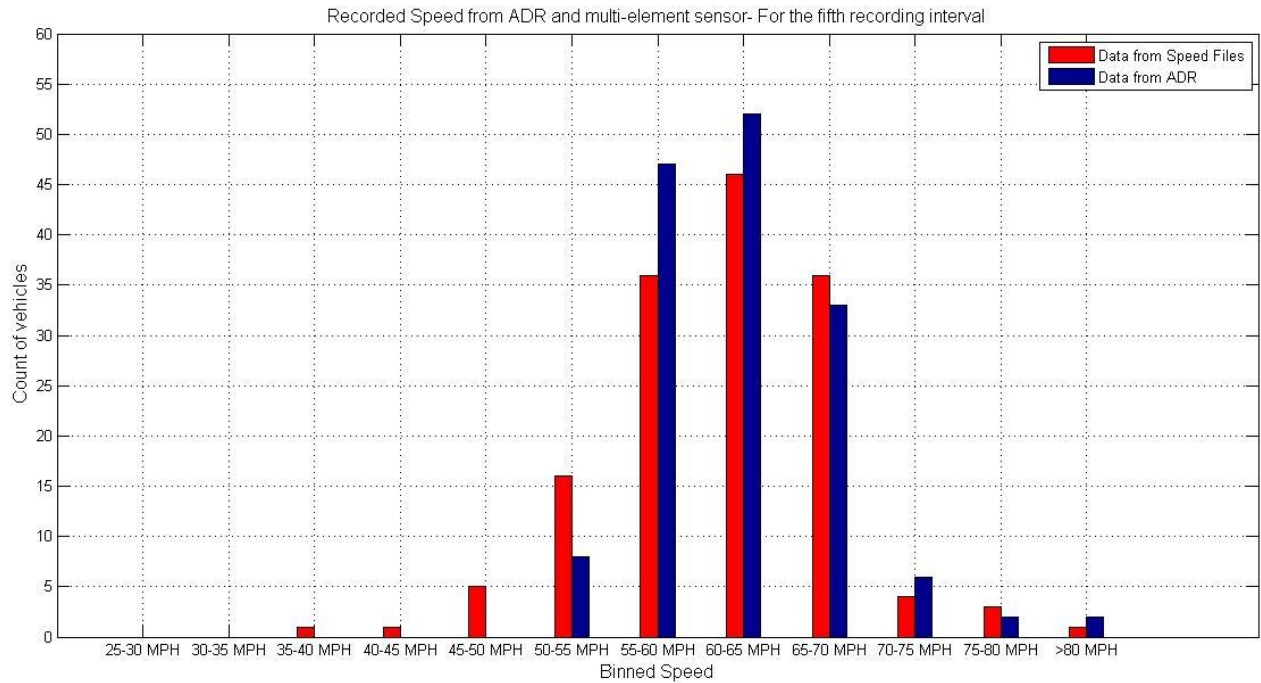


Figure 6-5. Speed distribution comparison between multi-element system and ADR for testing intervals 1 through 6

Notably, multi-element speed data in figure 6.5 was shifted by 2mph for all vehicles. This translates to an average of 0.35ft shift in distance between impacted elements. The reason for this adjustment was gaps

between consecutive sensors that averaged 0.35ft. Applying an average 2mph shift in speed compensated for the gaps resulting from multi-element sensor fabrication.

Figure 6.5 shows that both systems show similar distribution in terms of speed for all testing intervals, as well as only slight differences in vehicle count. Distribution in Figure 6.5 indicates extremely encouraging results, as it validates our speed calculation. Such results are essential for accurate system operability. A difference in vehicle count at a specific bin could result from data binning or error in width calculations from distance resolution when calculating width.

Axle spacing and vehicle length was calculated. Vehicle features were applied to the vehicle classification algorithm to generate classification results shown in Tables 6.2 and 6.3. Table 6.2 corresponds to test intervals in which signal sampling rate was 5kS/s. Data was accumulated for approximately 2 hours, 30 minutes. Classification data shown in Table 3 was obtained from a test interval of approximately 10 minutes at a sampling rate at 10kS/s.

Table 6.2 shows that total achieved classification accuracy was 86.9% when compared to data generated from the video ground-truth system. The system scored 100 and 98.9% classification accuracy for motorcycles and passenger vehicles, respectively. Lower classification percentage for other classes can be attributed to a number of factors. For example classes 3, 4, and 5 have the same number of tires and axles. Thus, the algorithm can distinguish between vehicles based only on vehicle length. Likewise, false pulse detection can play a part in misclassifying heavier trucks. In this case, classification rate for the same interval was much lower at 70.6%. The short, 10-minute interval sample was simply not long enough to accurately reflect classification rate. See Table 6.3.

Table 6.2. Classification accuracy for AVC19 with 5kS/s testing round

	Video	Multi-element classification	Error
Class			
CI 1	5	5	0.00%
CI 2	453	458	-1.10%
CI 3	245	225	8.16%
CI 4	2	10	-400.00%
CI 5	32	16	50.00%
CI 6	27	42	-55.56%
CI 7	1	12	-1100.00%
CI 8	5	12	-140.00%
CI 9	99	77	22.22%
CI 10	1	3	-200.00%
CI 11	0	0	0.00%
CI 12	0	0	0.00%
CI 13	2	10	-400.00%
CI 14	0	0	0.00%
CI 15	0	2	0.00%

Table 6.3. Classification accuracy for AVC19 with 10kS/s testing round

	Video	Multi-element classification	Error
Class			
CI 1	0	0	0.00%
CI 2	53	55	-3.77%
CI 3	39	26	33.33%
CI 4	0	3	0.00%
CI 5	1	2	-100.00%
CI 6	1	5	-400.00%
CI 7	0	4	-1100.00%
CI 8	0	1	0.00%
CI 9	6	6	0.00%
CI 10	0	0	0.00%
CI 11	1	0	100.00%
CI 12	1	0	100.00%
CI 13	0	0	0.00%
CI 14	0	0	0.00%
CI 15	0	0	0.00%

Effects of changing angle on the system

The angle of deployment between sensor and traffic direction, i.e., θ , is an important parameter in the vehicle classification system. Effects of altering this angle will be addressed in this subsection. By decreasing the θ figure, fewer sensor elements are required to fabricate the sensor. Hence, a DAQ with fewer input channels is required, given that element length is fixed at 1.5ft. This advantage reduces system cost and ensures data processing. Also, less time is spent fabricating the multi-element sensor, and highway deployment is less complicated. Another advantage of decreasing the angle of the sensor in relation to traffic direction is reducing the probability of a malfunctioning element.

Decreasing θ will result in lower resolution when calculating vehicle width, primarily because fewer sensors are used in the system. A higher margin of error is possible when calculating width, which will effect speed and axle spacing calculations. However, from collected deployment data it is apparent that for many vehicles, especially trucks, multiple elements are impacted by wide or double tires. This implies that the system might work well with lower resolution relative to distance between elements. The system achieved respectable speed calculations even without utilizing the channel 3 signal, as indicated earlier in this chapter. This information implies the worthiness of investigating an increase in θ for future deployments.

Differences between single element and multi-element classification systems

The following table highlights advantages and disadvantages of single- and multi-elements systems.

Table 6.4. Comparison between single element and multi-element systems

	Single element system	Multi-element System
<i>Width detection</i>	Not Possible	Estimate vehicle width track
<i>Analog to digital conversion specifications</i>	Requires DAQ with one input channel	Requires DAQ with multiple input channels
<i>Ease of sensor packaging and road installation</i>	Easy to construct and deploy on highways	Challenging to construct and deploy on highways.
<i>Sensor disconnection tolerance</i>	Stop operation with damaged sensor.	Maintain operation even with damaged sensors but less resolution.
<i>Classification accuracy</i>	- Achieved up to 84.4% with average width algorithm. - Achieved up to 99% when using vehicle (W/L) ratio	Achieved up to 86.9%

Errors reported when processing multi-element data

This section explains the various type of errors encountered during the classification processing of the data obtained from the multi-element sensor design. Two different types of error were identified. They are similar to those identified during the single-element highway deployments. Description of the errors is described below.

Type 1 Error: Extra Pulses in Signal Data

Type 1 Error is indicated when pulses occur in signal data, although no vehicle is detected in video data. Thus, when processing raw signals and comparing them to video records, it can be assumed that signals could be the result of vehicles passing in an adjacent lane.

Type 2 Error: Distorted Pulses

Type 2 Error is indicated when the detected pulses associated with a particular crossing vehicle are fewer than expected. The primary reason is vehicle lane switching from the instrumented lane one to an adjacent one.

Conclusion

Vehicle classification accuracy is important for determining vehicle miles travelled (VMT) and designing roadways and highways that accommodate traveling passengers and goods transportation. Most US state departments of transportation employ a vehicle detection and classification system that uses two inductive loops combined with a piezoelectric sensor to measure vehicle speed, length, axle count, and axle spacing. However, this technology has been shown to misclassify motorcycles (class 1 vehicles) that leave a negligible roadway footprint. It is imperative to investigate other techniques and technologies to improve motorcycle classification.

This project proposed to develop a vehicle classification system to accurately classify motorcycles, as well as vehicles in the remaining 12 FHWA classes. The newly developed system utilizes a single- or multi-piezoelectric sensor(s) unconventionally placed diagonal to traffic flow. Sensor deployment tilt affords the system the ability to detect individual vehicle tires, estimate vehicle width, and potentially detect double tires used on trucks, in addition to tire width. The single-element design employs a single piezoelectric sensor, a one channel DAQ, and an embedded computer to process classification algorithms. The system is easy to deploy, simple to use, and inexpensive, although it offers less accurate speed estimates because of its inability to accurately estimate vehicle width. Alternately, the multi-element design uses several in-line piezoelectric sensors, a multi-channel DAQ, and embedded computer to process specific classification algorithms. This system is more tolerant of sensor failure and able to estimate vehicle width, thus more accurately estimate vehicle speed. However, the system is expensive and more complicated to use and deploy.

Various classification algorithms were developed for both single- and multi-element designs. Algorithms for the multi-piezoelectric system were implemented to determine tire count, tire spacing, vehicle width velocity, and pulse timing/duration, in addition to axle spacing and vehicle length, effectively leveraging the utility of the inductive loop technology. Tire-based parameters provide additional data that can be used to enhance classification accuracy, especially for class 1 motorcycles. Given this new technology, class 1 vehicles are easily detected primarily because they have only two tires, i.e., tire-initiated pulses are used to process feature extraction and vehicle classification. Vehicle width estimation provides accurate vehicle speed estimates. This outcome alone is beneficial, especially when considering that at least two inductive loops are required to measure vehicle speed. Classification accuracy using the multi-element sensor achieved up to 86.9% accuracy during highway deployments.

Algorithms developed for the single-piezoelectric sensor system were required to compensate for missing vehicle width data. Two algorithms were developed—one that uses an average vehicle width to calculate vehicle speed regardless of vehicle type and class, and another, more novel algorithm that uses the ratio of vehicle width over its length. This method does not require speed calculations and has proven superior in classification accuracy, even among vehicles with an equal number of tires. Accuracy ranged between 94.8% and 99.07% during highway deployment. Classification accuracy was calculated at 84.4% when average width is employed.

Implantation/Technology transfer

Single-element design and field testing portion of this project was published and presented at the International Transportation Systems Conference (ITSC) in September 2012 [17].

Single element system design and preliminary testing was presented at NATMEC 2012 under title: “Accurate Vehicle Classification Including Motorcycles Using Piezoelectric Sensors”.

Also, project progress was presented to the Oklahoma Department of Transportation (ODOT) on several occasions.

References

- [1] Xuemin Chen; Lianhe Guo ; Jingyan Yu ; Jing Li, “Evaluating Innovative Sensors and Techniques for Measuring Traffic Loads”, International Conference on Networking, Sensing and Control, 2008. ICNSC 2008. IEEE , 2008.
- [2] Janusz Gajda; Sroka, R.; Stencel, M. ; Wajda, A. ; Zeglen, T., “A Vehicle Classification Based on Inductive Loop Detectors”, IEEE Instrumentation and Measurement Technology Conference, 2001
- [3] Saowaluck Kaewkamnerd; Chinrungrueng, J. ; Pongthornseri, R. ; Dummin, S., “Vehicle Classification Based on Magnetic Sensor Signal,” Proceedings of the 2010 IEEE International Conference on Information and Automation, pp. 935-939, June 2010.
- [4] Sroka, R., “Data fusion methods based on fuzzy measures in vehicle classification process,” Proceedings of 21st IEEE Instrumentation and measurement Technology Conference, pp.2234-2239, May 2004.
- [5] Carlos Sun; Akoum, A.H. ; Chauvet, P., “Inductive Classifying Artificial Network for Vehicle Type Categorization,” Computer-Aided Civil and Infrastructure Engineering, pp. 161-172, 2003.
- [6] Janusz Gajda; Sroka, R. ; Stencel, M. ; Wajda, A. ; Zeglen, T., “A Vehicle Classification Based on Inductive Loop Detectors”, IEEE Instrumentation and Measurement Technology Conference, 2001
- [7] Janusz Gajda; Sharma, P. ; Deshmukh, A., “Measurement of Road Traffic Parameters Using an Inductive Single-Loop Detector”, 1997
- [8] Wang, Y. and Nihan, N., ”Can Single-Loop Detectors Do the Work of Dual-Loop Detectors?,” Journal of Transportation Engineering, 129(2), 169–176, 2003
- [9] Soner Meta and Muhammed G. Cinsdikici, “Vehicle-Classification Algorithm Based on Component Analysis for Single-Loop Inductive Detector,” IEEE Transactions on Vehicular Technology, VOL. 59, NO. 6, pp. 2795-2805, 2010.
- [10] Wenbin Zhang; Qi Wang; Chunguang Suo, “A Novel Vehicle Classification Using Embedded Strain Gauge Sensors,” Sensors – Open Access Journal, 8, pp. 6952-6971, 2008.
- [11] Ravneet Bajwa; Rajagopal, R. ; Varaiya, P. ; Kavalier, R., “In-Pavement Wireless Sensor Network for Vehicle Classification,” Information Processing in Sensor Networks (IPSN), pp. 85-96, 2011.
- [12] Golla, P. R.; Mukherjee, A. ; Harvey, B., "Extruded segmented sensor for road traffic classification," Proceedings of IEEE Southeastcon, pp.1, 5, 4-7, 2013
- [13] Yan, L.; Fraser, M.; Elgamal, A.; Fountain, T.; Oliver, K., ”Neural Networks and Principal Components Analysis for Strain-Based Vehicle Classification.” J. Comput. Civ. Eng., 22(2), 123–132, 2008

- [14] L. Smith, A Tutorial on Principal Components Analysis, www.cs.otago.ac.nz/cosc453/student_tutorials/principal_components.pdf, 2002, Accessed September, 2013.
- [15] Sarbazi-Azad; M. M. Homayounpour; M. B. Menhaj, ” A Bayesian Network Based Approach for Data Classification Using Structural Learning” *Advances in Computer Science and Engineering, Communications in Computer and Information Science*, V 6, 2009
- [16] Kevin Murphy, “A Brief Introduction to Graphical Models and Bayesian Networks” <http://www.cs.ubc.ca/~murphyk/Bayes/bnintro.html>, 1998, Accessed September 2013
- [17] Rajab, S.A.; Othman, A.S.; Refai, H.H., "Novel vehicle and motorcycle classification using single element piezoelectric sensor," *15th International IEEE Conference on Intelligent Transportation Systems (ITSC)*, pp.496,501, 2012

Appendix A

In this appendix the Diamond Systems Helios computing system interface and related capabilities pertinent to this report are briefly explained.

The REECE device was initially developed as part of an Oklahoma Transportation Center (OTC) project funded in 2005-06. The goal of the project was to develop wireless access to Oklahoma Department of Transportation (ODOT) traffic data collection sites, enabling automatic vehicle classification (AVC) and weight-in-motion (WIM). The device was developed by PI Dr. Refai and his research team at the University of Oklahoma-Tulsa. The REECE is able to access a cellular network using either a 3G or 4G wireless modem, and then transfer data back and forth to servers in real time. Diamond Systems Prometheus served as the basis for the computing system; development advanced to incorporate the new generation of Helios.

Helios is an embedded system designed by Diamond Systems. See figure A.1. The compact, embedded computer is able to execute a number of operating systems, including Linux.

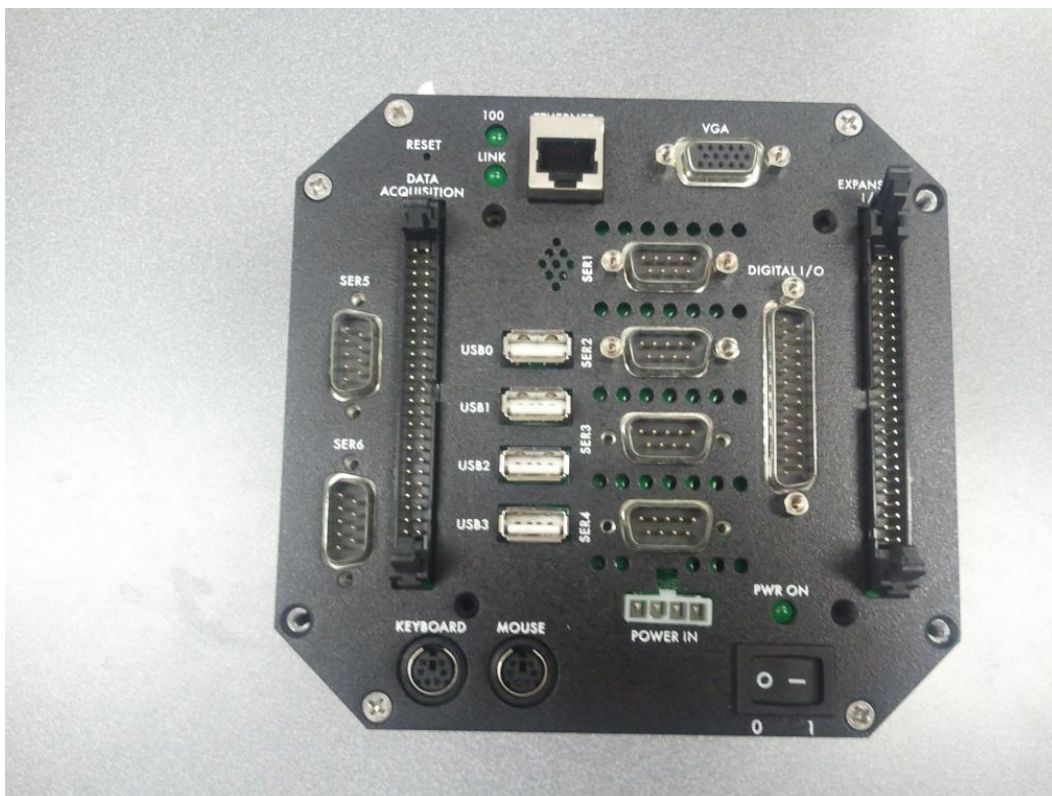


Figure A. 1. Helios computing system

Helios has an 800 vortex86DX CPU and is equipped with six VGA ports; PS/2 mouse and keyboard ports; RS-232 ports; four USB ports; 40 digital programmable I/O lines; four analog outputs; and Ethernet port with 10/100 Ethernet circuit integrated into the processor. Most important among Helios I/O ports is the 16 analog inputs, further detailed below.

Helios includes a built-in DAQ unit that can operate with 16 single ended (SE) channels or 8 differential channels. Helios DAQ scans input channels sequentially and has a maximum sampling rate of 250kS/s, although this rate is divided among input channels when more than one channel is used. For example, when using 16 SE input channels, the rate drops to 15.625kS/s.

Signal input is connected to Helios DAQ through a 50-pin male header on the I/O module. The header is comprised of all 16 analog input channels; four analog outputs; grounds; voltage out; and digital I/Os. See figure A.2.

DIO A0	1	2	DIO A1
DIO A2	3	4	DIO A3
DIO A4	5	6	DIO A5
DIO A6	7	8	DIO A7
DIO B0	9	10	DIO B1
DIO B2	11	12	DIO B3
DIO B4	13	14	DIO B5
DIO B6	15	16	DIO B7
DIO C0	17	18	DIO C1
DIO C2	19	20	DIO C3
DIO C4 / Gate 0	21	22	DIO C5 / Gate 1
DIO C6 / Clk 1	23	24	DIO C7 / Out 0
Ext Trig	25	26	Tout 1
+5V Out	27	28	Dground
Vout 0	29	30	Vout 1
Vout 2	31	32	Vout 3
Aground (Vout)	33	34	Aground (Vin)
Vin 0	35	36	Vin 8
Vin 1	37	38	Vin 9
Vin 2	39	40	Vin 10
Vin 3	41	42	Vin 11
Vin 4	43	44	Vin 12
Vin 5	45	46	Vin 13
Vin 6	47	48	Vin 14
Vin 7	49	50	Vin 15

Figure A. 2. DAQ I/O connector

The aforementioned features render the REECE device Helios an appealing platform for the development of a vehicle classification embedded system. It is currently deployed at 80 ODOT data collection sites, making the deployment of the single/multi-element classifier at these sites inexpensive, thus feasible.

Appendix B

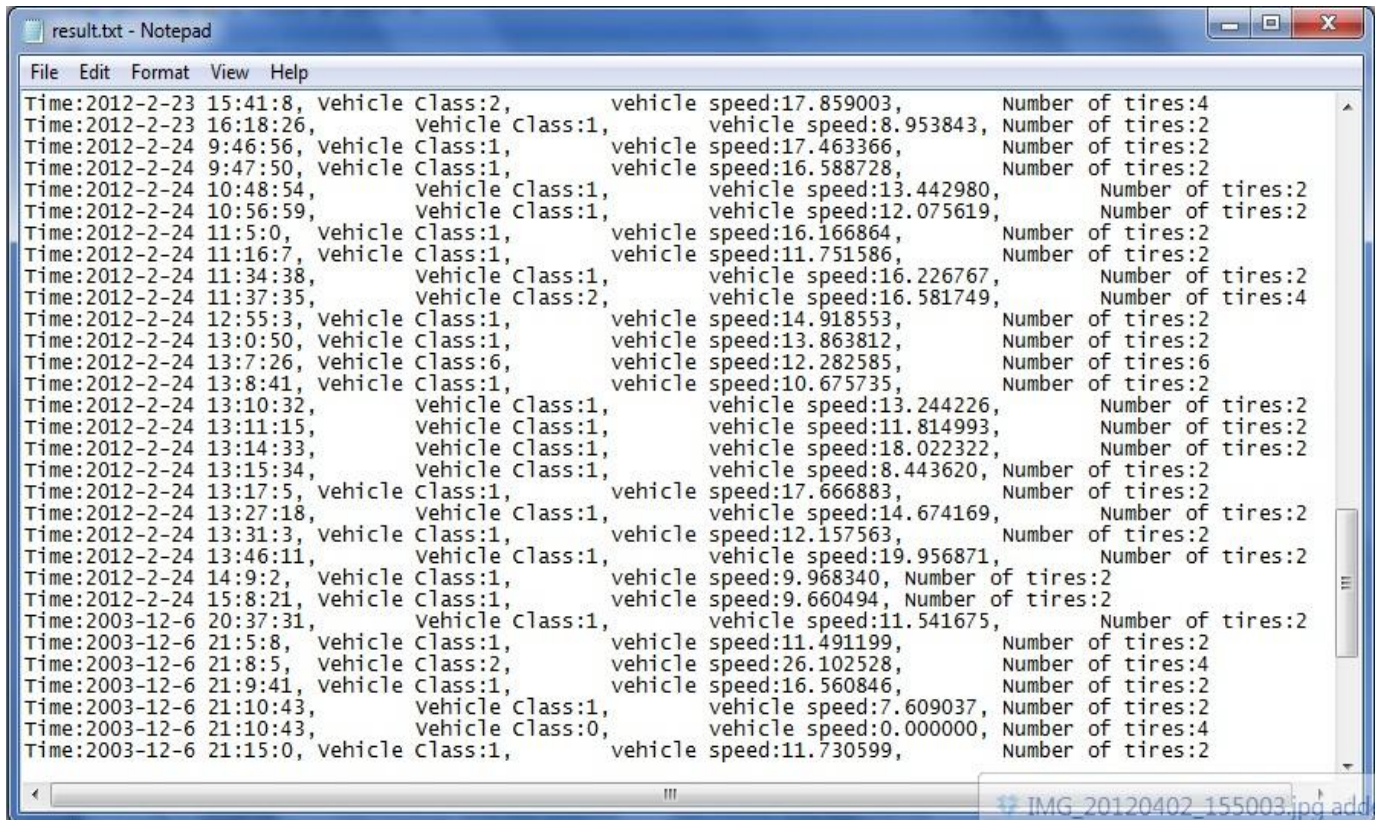
This appendix shows the procedure by which a new REECE device is added to the Linux server VPN network. It is assumed that the REECE device is working and has Internet connection.

- REECE will continue to attempt to connect with server.
- On server, check for REECE connection and obtain its public IP address: `tail -f /var/log/secure`
- Connect to REECE using Linux terminal software putty or any other terminal software
- Generate new RSA keys
- Secure copy (scp) public key to the server
- On server, add REECE name to the list of users
- Give user (REECE) permission to create VPN connection
`Echo '<name> ALL=NOPASSWD: /usr/sbin/pppd call <name>' >> /etc/sudoers`
- Make new file in `"/etc/ppp/peers/"` named as REECE user. Then file the VPN connection options and parameters for this user and the specific VPN network address assigned to the REECE.
- Install public keys on server and make REECE user as their owner:
`cp /PATHofPublicKey/id_rsa.pub /home/<name>/.ssh/authorized_keys2`
`chown <name>:<name> -R /home/<name>`

Appendix C

This appendix describes the algorithm output developed program for the REECE device. When executed, the program continuously processes sensor data, looking for a passing vehicle. Per-vehicle records are reported on screen and saved on the REECE memory. These include passing time, date, vehicle class, velocity, and number of tires. See figure C.1 for an example of reported output. A connection is initiated to the REECE device either directly to its public IP address or through a VPN connection from a server. During the session, the program can be initiated and stopped, and vehicles can be detected as they pass. The output has the following parameter:

- Time and date of record
- Vehicle class
- Vehicle speed
- Number of tires



```
File Edit Format View Help
Time:2012-2-23 15:41:8, vehicle class:2, vehicle speed:17.859003, Number of tires:4
Time:2012-2-23 16:18:26, vehicle class:1, vehicle speed:8.953843, Number of tires:2
Time:2012-2-24 9:46:56, vehicle class:1, vehicle speed:17.463366, Number of tires:2
Time:2012-2-24 9:47:50, vehicle class:1, vehicle speed:16.588728, Number of tires:2
Time:2012-2-24 10:48:54, vehicle class:1, vehicle speed:13.442980, Number of tires:2
Time:2012-2-24 10:56:59, vehicle class:1, vehicle speed:12.075619, Number of tires:2
Time:2012-2-24 11:5:0, vehicle class:1, vehicle speed:16.166864, Number of tires:2
Time:2012-2-24 11:16:7, vehicle class:1, vehicle speed:11.751586, Number of tires:2
Time:2012-2-24 11:34:38, vehicle class:1, vehicle speed:16.226767, Number of tires:2
Time:2012-2-24 11:37:35, vehicle class:2, vehicle speed:16.581749, Number of tires:4
Time:2012-2-24 12:55:3, vehicle class:1, vehicle speed:14.918553, Number of tires:2
Time:2012-2-24 13:0:50, vehicle class:1, vehicle speed:13.863812, Number of tires:2
Time:2012-2-24 13:7:26, vehicle class:6, vehicle speed:12.282585, Number of tires:6
Time:2012-2-24 13:8:41, vehicle class:1, vehicle speed:10.675735, Number of tires:2
Time:2012-2-24 13:10:32, vehicle class:1, vehicle speed:13.244226, Number of tires:2
Time:2012-2-24 13:11:15, vehicle class:1, vehicle speed:11.814993, Number of tires:2
Time:2012-2-24 13:14:33, vehicle class:1, vehicle speed:18.022322, Number of tires:2
Time:2012-2-24 13:15:34, vehicle class:1, vehicle speed:8.443620, Number of tires:2
Time:2012-2-24 13:17:5, vehicle class:1, vehicle speed:17.666883, Number of tires:2
Time:2012-2-24 13:27:18, vehicle class:1, vehicle speed:14.674169, Number of tires:2
Time:2012-2-24 13:31:3, vehicle class:1, vehicle speed:12.157563, Number of tires:2
Time:2012-2-24 13:46:11, vehicle class:1, vehicle speed:19.956871, Number of tires:2
Time:2012-2-24 14:9:2, vehicle class:1, vehicle speed:9.968340, Number of tires:2
Time:2012-2-24 15:8:21, vehicle class:1, vehicle speed:9.660494, Number of tires:2
Time:2003-12-6 20:37:31, vehicle class:1, vehicle speed:11.541675, Number of tires:2
Time:2003-12-6 21:5:8, vehicle class:1, vehicle speed:11.491199, Number of tires:2
Time:2003-12-6 21:8:5, vehicle class:2, vehicle speed:26.102528, Number of tires:4
Time:2003-12-6 21:9:41, vehicle class:1, vehicle speed:16.560846, Number of tires:2
Time:2003-12-6 21:10:43, vehicle class:1, vehicle speed:7.609037, Number of tires:2
Time:2003-12-6 21:10:43, vehicle class:0, vehicle speed:0.000000, Number of tires:4
Time:2003-12-6 21:15:0, vehicle class:1, vehicle speed:11.730599, Number of tires:2
```

Figure C. 1. Vehicle per vehicle reported output.